

402182

AD No.   
ASTIA FILE COPY

(1)

EASTMAN KODAK COMPANY  
APPARATUS AND OPTICAL DIVISION

ASTIA  
RECEIVED  
APR 11 1966

ASTIA  
ASTIA Cont. Pr.

*Wj.*

8,10

July 8 1960  
Copy No. 2

(10) 87p. incl. illus.  
- tables, 6 refs.

(15) 280 500

(17) Semi-Annual Report.  
~~on a~~

(18) see next page

(16) Space Background Study

(12) Contract DA-30-069-ORD-2803

(11) EK/ARD ED-442

(10) N.A.

(9) N.A.

(8) N.A.

For the

Army Rocket and Guided Missile Agency  
U. S. Army Ordnance Missile Command  
Redstone Arsenal, Alabama

Submitted by

Eastman Kodak Company  
Apparatus and Optical Division, Lincoln Plant  
Rochester, New York

PREPARED BY

187  
Charles Gramm, Engineer  
Eastman Kodak Company

on 2/26/52.  
William Haynie, Engineer  
Eastman Kodak Company

Walter E. Mitchell  
Ohio State University  
Research Foundation

Philip Barnhart  
Ohio State University  
Research Foundation

REVIEWED BY

E. D. McAlister  
E. D. McAlister, Assistant Superintendent  
Research & Development - Missile Subsystems  
Department 421, Lincoln Plant

APPROVED BY

E. H. McLaughlin  
E. H. McLaughlin, Superintendent  
Research & Development - Missile Subsystems  
Department 421, Lincoln Plant



ABSTRACT

A theoretical model of the infrared stellar background is presented, based on a blackbody extrapolation of stellar data for the visible and near infrared regions. Stellar magnitudes are limited by the irradiance of a 2-square-meter 300°K target at 500 nautical miles. The total number of interfering stars decreases from the order of one hundred thousand in the visual region to only several hundred for the infrared beyond 7.5 microns. Star maps of the celestial sphere and a table of 185 stars in the order of their infrared magnitudes are included.



## TABLE OF CONTENTS

	<u>Page</u>
Title Page	1
Signature Page	2
Abstract	3
Table of Contents	4
List of Illustrations	5
List of References	7
I. Introduction	9
II. Technical Summary	11
III. Technical Approach	14
IV. Literature Survey	16
V. Target and Stellar Infrared Irradiance	29
VI. The Infrared Stellar Background and a System of Infrared Magnitudes	35
VII. A Program for Infrared Astronomical Photometry	47
Appendices	
A. Bandpass Characteristics of Magnitude Scales	64
B. Comparison of Color Indices in the Infrared	77
C. List of Stars Brighter Than Apparent Visual Magnitude +6.0 and Z-Magnitude 0.0	79
Distribution List	86

LIST OF ILLUSTRATIONS

<u>Figure</u>	<u>Title</u>	<u>Page</u>
1	Irradiances of 300°K Satellites in Free Space and Irradiances Limited by the Transmittance of One Air Mass	31
2	Limiting Visual Magnitude for Stars $\frac{1}{10}$ Target Intensity	33
3	All Stars Brighter than Apparent Visual Magnitude +3.0 Plotted on an Equal Area Project	41
4	All Stars Brighter than Apparent Visual Magnitude +3.0 and Brighter than Apparent 3-Magnitude 0.0	42
5	All Stars Brighter than Apparent Visual Magnitude +6.0 Detectable in the Z-Region 7.5 to 13.5 Microns	43
6	All Stars Brighter than Apparent Visual Magnitude +6.5 in the Region of the Sky Between Right Ascension 1h 40 <sup>m</sup> and 6h 20 <sup>m</sup> and Declinations $\pm 60^\circ$	44
7	All Stars in the Same Region as Shown in Figure 6 Brighter than Apparent Z-Magnitude 0.0	45
8	IR Stellar Photometer Optical System	50
9	Limiting Stellar Magnitudes for Various Infrared Detectors and the 60-inch Perkins Reflector	51
10	Spectral Transmittance of a 2.0-2.4 Micron Multilayer Interference Filter	53
11	Spectral Transmittance of a 8.0-13.0 Micron Multilayer Interference Filter in Combination with Barium Fluoride Windows	54
12	Product Curves for a 2000°K Blackbody in the Lead Sulfide 2.0-2.4 Micron Region Including the Effect of Atmospherics	55

LIST OF ILLUSTRATIONS (Cont'd.)

<u>Figure</u>	<u>Title</u>	<u>Page</u>
13	Product Curves for 6000°K Blackbody in the Lead Sulfide 2.0 to 2.4 Micron Region Including the Effect of Atmospherics	56
14	Product Curves for 2000°K Blackbody in the Thermocouple 8-13 Micron Region Including the Effect of Atmospherics	57
15	Product Curves for 6000°K Blackbody in the Thermocouple 8 to 13 Micron Region Including the Effect of Atmosphere	58
16	Comparison of Infrared Color Indexes	78

## REFERENCES

1. W. Coblentz, Lick Obs. Bull., 8, 104, 1915.
2. W. Coblentz, Scientific Papers, U. S. Bur. of Standards, 17, 725, 1922.
3. E. Pettit and S. Nicholson, PASP, 34, 181, 1922.
4. W. Coblentz, Journal Franklin Inst., 199, 785, 1925.
5. E. Pettit and Nicholson, Ap. J. 68, 279, 1928.
6. C. G. Abbot, Ap. J. 69, 293, 1929.
7. H. H. Plaskett, Pub. Dom. Ast. Obs., 2, 242, 1932.
8. J. S. Hall, Ap. J., 79, 145, 1934.
9. A. L. Bennett, Pub. of AS, 8, 209, 1935.
10. C. Hetzler, Ap. J., 83, 372, 1936.
11. C. Hetzler, Ap. J., 86, 509, 1937.
12. J. Stebbins and A. E. Whitford, Ap. J., 87, 237, 1938.
13. A. Adel, Ap. J., 89, 1, 1939.
14. W. M. H. Greaves, M. N. 100, 188, 1940.
15. J. Stebbins, A. E. Whitford, G. Kron, J. Hall and C. S. Beale,  
PASP, 52, 235, 1940.
16. E. Pettit, Ap. J., 91, 159, 1940.
17. D. Barbier and D. Chalonge, Ann. d'Astrophys. 4, 30, 1941.
18. J. S. Hall, Ap. J., 94, 71, 1941.
19. J. S. Hall, Ap. J., 95, 231, 1942.
20. J. Stebbins and A. E. Whitford, Ap. J., 98, 20, 1943.
21. J. Stebbins, Ap. J., 101, 47, 1945.

22. D. Chalonge and R. Canavaggia, *Ann. J'Astrophys.*, 9, 143, 1946.
23. H. F. Weaver, *Pop. Ast.*, 54, 504, 1946.
24. J. Stebbins and A. E. Whitford, *Ap. J.*, 106, 235, 1947.
25. G. Kron, *PASP*, 59, 173, 1947.
26. R. Canavaggia, D. Chalonge, M. Egger-Moreau, and H. Oziol-Pelley, *Ann. d'Astrophys.*, 13, 355, 1950.
27. R. Michard, *Bull. Astronom. Neth.*, 11, 227, 1950.
28. P. Fellgett, *M. N.* 111, 537, 1951.
29. L. Larmore, *JOSA*, 44, 827, 1951.
30. W. Sinton, *Phys. Rev.* 86, 424, 1952.
31. L. Larmore, "Infrared Radiation From Celestial Bodies," Rand Research Memo RM-793-1 June 1952.
32. M. Minnaert, Chapter III in "The Sun" Edited by G. P. Kuiper, Chicago University Press, 1953.
33. I. N. Jarosevcev, *Isv. Akad. Nauk, USSR, Ser. Geofic*, 8, 984, 1956.
34. D. Labs, *Sitzgsber, Heidelberg, Akad. Wiss.*, Springer 1957.
35. D. J. Lovell and G. R. Miczaika, "An Infrared Technique for Stellar Photometry," from the Present and Future of the Telescope of Moderate Size, University of Pennsylvania Press, 1958.
36. C. deJager, *Hand. der Phys.* 52, 143, 1959.
37. L. Goldberg, and A. K. Pierce, *Hand. der Phys.* 52, 1, 1959.
38. M. Lunel, *Ann. d'Astrophys.* 23, 1, 1960.

## I. INTRODUCTION

The importance of the role of optical sensors in the development of systems for space defense, surveillance, and navigation has been generally recognized. Optical equipment for space applications potentially offers high resolution and long range detection capability coupled with an overall relatively light weight and small size.

It will be appreciated, however, that the great number of optically detectable objects in a typical space background will create real confusion in optical sensing systems unless suitable discrimination techniques are employed. Spatial and spectral filtering techniques are under development as well as methods of indicating moving targets. However, it has been found that detailed information on the space background, especially in the infrared, is lacking to the designer of space defense systems. Unless this information is made available, the development and design of suitable optical systems for the detection and tracking of satellites, space vehicles, and missile nose cones will be seriously delayed. Only when the characteristics of the background have been established may optimum methods of discrimination be brought to bear.

The Eastman Kodak Company has been given the assignment, under contract with the Army Rocket and Guided Missile Agency, to investigate the magnitude of the stellar background problem and methods of solution to the problem in relation to space defense. Emphasis has been placed on the infrared spectral region, due to the requirements of passively detecting relatively cold (300°K) targets at long range. The delineation of the

stellar background has become a problem of locating the stars which produce irradiance comparable to that from the targets at relatively long infrared wavelengths (to 20 microns).

Specifically the contract requirements are as follows:

- (1) Collect existing astronomical data on stellar brightness, spectral type, and distribution on the celestial sphere. Sub-contracting to suitable university groups should be the preferred method of gathering this data.
- (2) Present the collected data in a form which will show the nature, extent, and severity of the space background problems as faced by anti-missile and other space defense systems using optical sensors.
- (3) Study all possible methods of alleviating the space background as found to exist. These methods will be applicable to optical sensor systems as used in space defense missile systems, will cover all optical wavelengths, and will consider sensor locations from sea level to free space.
- (4) Indicate additional astronomical observations required, and make recommendations as to desirable methods of background alleviation.

An amendment was later added stating that:

The contractor shall perform experiments which will be indicative of the propriety of assumptions and extrapolations devised under part (2). Whenever possible, existing equipment will be utilized.

The Ohio State University Research Foundation has joined with the Eastman Kodak Company under sub-contract to aid in this investigation, giving particular attention to the collection and presentation of astronomical data. This report is a summary of the effort of the two organizations.

## II. TECHNICAL SUMMARY

The Eastman Kodak Company, under a current contract with the Army Rocket and Guided Missile Agency, was assigned to collect existing astronomical data and present this collected data in a form which would show the nature, extent, and severity of the space background problems as faced by anti-missile and other space defense systems employing optical sensors. Concurrently, the Ohio State University Research Foundation was engaged by subcontract to jointly pursue the problem.

Emphasis has been placed on the detection of targets by means of their own thermal radiation rather than by means of reflected solar energy. The targets of interest are relatively cold bodies ( $300^{\circ}\text{K}$ ) with most of their radiated energy concentrated in the infrared region. Accordingly, effort has been directed toward characterization of the stellar background in the infrared.

An intensive literature search for data on stellar radiation beyond the near infrared yielded very little information. This was not surprising in view of the fact that long wavelength detectors with sufficient sensitivity to obtain the desired information have only recently become available. Lacking experimental data, we have assumed that stellar bodies behave as classical blackbody radiators, and we have extrapolated far into the infrared from the data available.

Target characteristics, as given, are a skin temperature of  $300^{\circ}\text{K}$ , a projected area of 2 square meters, an average thermal emissivity of 0.5, and a distance of 500 nautical miles. For a target to

background contrast of 10 to 1, the limiting stellar irradiance will range from  $2.2 \times 10^{-18}$  watts/cm in the 3 to 4 micron region to  $5.6 \times 10^{-16}$  watts/cm<sup>2</sup> in the 7.5 to 13.5 micron region.

It has been tacitly assumed that these irradiances are detectable, and the limiting stellar visual magnitudes were calculated for each spectral class. The desirability of using the longer wavelength bands to minimize stellar backgrounds is immediately apparent. In the region beyond 8 microns, none of the blue giants or super-giants appears and cool red stars are evident only down to and including about 8th magnitude. Furthermore, since the hot blue stars are found primarily in the plane of our galaxy, when these stars are filtered out, the distribution of stars on the celestial sphere becomes more nearly random. This in itself should simplify the additional discrimination required to remove the contributions of the remaining stars.

The results obtained from this extrapolation are very striking in that the total number of interfering stars decreases from the order of a hundred thousand to the order of several hundred when the observing instrument is shifted from the visible region to the infrared region beyond 7.5 microns.

These encouraging results from the study are, however, based on the following two assumptions:

1. The stars radiate at longer infrared wavelengths as they would if they were blackbodies at the temperature deduced from their radiation in the visual region of the spectrum.
2. The "infrared stars", that is, those sources which are too cool to radiate measurably in the visible, are not present in sufficient number to significantly affect the conclusions drawn from the data available for the visible stars.

In order to verify these two assumptions, it has been proposed to the Army Rocket and Guided Missile Agency that a planned program of infrared stellar photometry be initiated to provide a description of the space background on a more sound basis.

### III. TECHNICAL APPROACH

Joint discussions between representatives from the Eastman Kodak Company and Ohio State University have resulted in an approach designed to best meet the contract requirements.

The details of the technical approach follow:

1. Pursue a literature search to determine what measurements have been made on the infrared energy of stars and other celestial objects.
2. Investigate astronomical magnitude systems in order to devise an appropriate system of magnitudes for the intermediate and far infrared.
3. Compute the infrared irradiance of 300° Kelvin sources at desired ranges to establish magnitude limits for celestial emitters in the spectral regions under study.
4. Study the spectral distribution of solar radiation from the ultraviolet to the radio regions and compare this distribution with the black body curve for the photospheric temperature. Study the bolometric corrections required for radiation of all stellar spectral types.

5. Compute the infrared magnitudes for stars of all spectral classes to the magnitude limits.
  - a. Determine the infrared color indices for various spectral types.
  - b. Tabulate the major visible objects in the sky and their apparent infrared magnitudes.
  - c. Present the distribution of the brightest infrared objects which are apparent on the celestial sphere.
  
6. Outline a program for observations of astronomical sources at infrared wavelengths in order to verify by direct measurement the theoretical assumptions and computations.
  
7. Implement the measurement program of infrared stellar photometry with suitable optical and electronic instrumentation.

#### IV. LITERATURE SURVEY

##### SUMMARY

To the present time, the only detectors of infrared radiation which have been turned on astronomical sources of radiation to any extent, are the thermocouple, lead sulfide and golay cell. The brightness of approximately 70 stars has been measured in the lead sulfide region but, beyond a wavelength of about 3 microns, the only sources studied have been the sun, moon, Mars and Venus. In regard to the electromagnetic spectrum beyond 20 microns, many astronomical sources have been detected by radio techniques at wavelengths around one meter and longer but, short of one centimeter, the sun has been the only source studied.

##### A. INTRODUCTION

Determination of the spectral energy distribution of stellar objects, including the sun, is greatly complicated by the extensive and variable opacity of the earth's atmosphere and only limited portions of the spectrum can be observed from the surface of the earth. However, the technology of space exploration is on the verge of providing complete coverage of the spectrum by means of satellite observation.

Complete observations of the energy distribution of a star's spectrum are therefore not yet available. On the other hand, measurements of the energy distribution in limited regions of the spectrum have been used for some time to obtain temperatures of stellar sources. Four types of temperatures are encountered in astrophysical studies. They are:

1. Black-body Temperature - the temperature of a black body having the same specific emission at some wavelength,  $\lambda$ , as the star.

2. Radiation Temperature - the temperature of a black body having the same specific emission in some wavelength range,  $\lambda_1$  to  $\lambda_2$ , as does the star.
3. Effective Temperature - the temperature of a black body having the same total emission as a star.
4. Color Temperature - the temperature of a black body having the same distribution of relative intensity as the star.

Determination of the first three temperatures listed requires knowledge of the absolute energy emitted per unit area of the star. Since absolute energy measurements are available only for the sun, it is the only star for which all four temperatures can be determined directly. The usually observed quantity for the stars is the radiation intensity which contains the effects of the unknown radius and distance of the star as well as that of the transmission through the earth's atmosphere and of the selective sensitivity of the detecting apparatus.

It has been known for some time that a single temperature can not be assigned to the entire solar energy distribution. The black-body and especially the color temperatures derived from the energy curve vary with the wavelength of the region in which they are determined. From the measured values of the solar constant, the effective temperature for the sun is  $T_e - 5713^\circ\text{K}$ . The form of the distribution in the neighborhood of the maximum energy corresponds to a color temperature of about  $7000^\circ\text{K}$ ., while the gradient to the ultraviolet side of the maximum leads to color temperatures lower than  $5000^\circ\text{K}$ .

In cases other than the sun, one is generally confined to the determination of color temperature from spectrophotometric measurements of intensity gradients. For distant stars, these results may be greatly affected by interstellar absorption which always tends to lower the observed temperature (i.e. to redden the star).

#### B. INFRARED OBSERVATIONS

The search for available observations beyond 1.0 micron in the near infrared has led to the conclusion that observers in this field have become discouraged due to the extreme insensitivity of available detectors. Most of the information available in energy distribution at wavelengths longer than 1.5 microns comes from non-selective detectors; i.e., thermocouples, radiometers, pyrhelimeters, etc.

One of the earliest workers in infrared astronomical measurements was Coblentz (Reference 1) who in 1914 used very sensitive vacuum thermocouples of his own construction to make an extensive series of thermoelectric observations of radiation from 125 celestial objects, among them 110 stars, some of which were as faint as visual magnitude 6.7. Coblentz also made very crude spectrophotometric measurements for a number of these stars by determining the ratio of the total amount recorded with and without a water cell placed before the thermocouple. The water cell was one centimeter thick with quartz windows, and only transmitted radiation shorter than 1.4 microns. With the cell in place, radiation from 0.3 to 1.4 microns

was observed, and without the cell, the upper limit was established by the infrared response of the thermocouple.

By means of water cell transmission methods, the first of their kind, Coblentz showed that the total radiation emitted by blue stars has about twice as high a percentage of visible radiation as yellow stars, and about three times as high a percentage as red stars.

In 1921 Coblentz made further thermal radiation measurements at Lowell Observatory where he investigated the possibility of obtaining the spectral energy distribution of stars by means of filters, used either singly or in combination. With these filters it was possible to isolate the following spectral regions: 0.3 to 0.43 microns, 0.43 to 0.60 microns, 0.60 to 1.4 microns, 1.4 to 4.1 microns, and 4.1 to 10.0 microns (Reference 2).

Pettit and Nicholson about this time made observations on 13 stars using a thermocouple attached to the 100 inch Hooker telescope at Mt. Wilson (Reference 3). They defined the radiometric magnitude of a star as the magnitude of an A0 star which would give the same galvanometer deflection. The heat index was defined as the visual magnitude ( $m_V$ ) minus the radiometric magnitude ( $m_T$ ). On the basis of these measurements, Pettit and Nicholson tabulated for the 13 stars the visual and radiometric magnitudes, and obtained heat indices ( $m_V - m_T$ ) as high as 8 magnitudes for very late dwarf stars.

Later results published in 1928 provided the magnitudes of 128 stars without a terrestrial atmosphere, their total radiation reaching the solar system and the computed bolometric magnitude for each star (Reference 5). Temperatures and diameters computed from the radiometric results are given for stars of special interest. The heat index shows distinct branches between stellar classes F5 and A0, the giant stars showing greater values and therefore lower temperatures than the dwarfs. The plot of the heat index against water cell absorption shows that the red stars deviate from the black-body conditions.

Again A0 stars were selected for the determination of the zero points because the photographic and visual magnitudes are equal for this spectral class. The heat index, like the color index, is therefore zero for these stars.

In 1928, Abbot made measurements of intensity distribution in the spectra of some bright stars, (Reference 6). He used a fly's-wing radiometer attached to the coude spectrograph of the Mount Wilson 100-inch telescope. The observations covered the spectral range 0.42 to 2.24 microns. Little quantitative information came from the investigation but the curves for different stars behaved much as would be expected from the Wien Law.

J. S. Hall compared early type stars directly with a standard lamp and found some infrared excess occurring beyond the Paschen limit, indicating that hydrogen-continuous absorption, at other than the Balmer limit, plays a role in shaping the energy distribution curves of the early type stars (Reference 8).

Fellgett, in 1951, made lead-sulfide measurements on 50 stars and thereby provided their PbS magnitudes and indices which, in turn, generally agree with black-body magnitudes computed for similar temperatures (Reference 28).

In 1952, L. Larmore of the Rand Corporation published a now unclassified report on the infrared radiation of celestial bodies within the lead sulfide and bolometer response regions to 13.5 microns (Reference 31). This work was based on an analysis of black-body emission in the infrared as a function of temperature and the spectral response of the receivers. Not considered were the effects of atmospheric absorption which would introduce a significant change in the computed values of effective irradiance.

More recently, Lovel and Miczaika have shown the usefulness of lead sulfide for stellar photometry in the infrared with the effective radiation including atmospheric absorption (Reference 35). A photometer system is discussed which employs a two element lead sulfide cell and a narrow bandwidth RC filter following a phase-sensitive detector. No provision has been made for measurements beyond 3.5 microns.

A system of this type has been introduced at the Harvard College Observatory and can be used with the 61-inch reflector. As yet, measurements obtained by this photometer have not been reported.

M. Lunel, in 1960, has reported on lead sulfide observations of 61 stars (Reference 38). Her results agree quite well with Fellgett and support the belief that the radiation in the PbS region bears nearly the same relation to the visible region as does black-body radiation.

C. SOLAR RADIATION DISTRIBUTION

The most profitable investigations of stellar energy distributions have been made in the observable spectral regions of the sun. These readily observable regions of the solar spectrum are the visual, from about 0.4 to 2.5 microns, and the radio region extending from 3 millimeters to 10 meters.

The work directed toward obtaining the energy distribution in the visual region has been summarized by Goldberg and Pierce in 1959 (Reference 37).

An accurate determination of the energy distribution in the sun's spectrum resulted from the work started by Langley in 1883 at the Allegheny Observatory and the Smithsonian Institution, Washington, and by Wilsing in 1905 at the Astrophysical Observatory at Potsdam. Wilsing compared

the sun's radiation to that of a black body in the interval 0.45 to 2.1 microns. In the visual region of the spectrum he found that the energy distribution corresponded to a color temperature of 6300°K.

To carry out Langley's program, Abbot, Aldrich and Fowle obtained bolograms of the solar energy curve from 0.34 to 2.4 microns at different air masses and, from these, computed the energy distribution of the incident solar radiation outside the earth's atmosphere. Refinements of the method of Langley as well as advancing techniques of measurement have led to greatly improved values for the solar energy distribution in the visual and near infrared region. Johnson (1954) gives values for the solar energy distribution from 0.2 to 7.0 microns.

In the visual region it is found that absorption lines crowd the spectrum between 0.4 and 0.5 micron, but beyond the magnesium group at 0.518 micron they decrease. When 0.60 micron is reached, many intervals can be found which are relatively free of line absorption, and here the continuum can be well established even with low dispersion spectrometers. In the region 0.42 to 0.66 micron a specific attempt was made by Plaskett (1932) to measure the monochromatic intensity at selected wavelengths chosen to be as free as possible of Fraunhofer lines (Reference 7). Since his spectral resolution was high, the true continuum was closely defined. He finds a color temperature of from 6200° to 7000°K., somewhat more than the effective temperature, obtained from the total emission, of 5713°K.

Chalonge and his co-workers approached the problem by assuming in the two intervals, 0.36 to 0.50 micron and 0.32 to 0.36 micron which are divided by the Balmer limit, that separate black-body color temperatures could be assigned (Reference 22). From their measurements they obtained a temperature of 7130°K for the region to the longer wavelengths and a temperature of 5900°K for the shorter wavelengths.

Michard re-evaluated some of Pettit's measures (1940) from the point of view of correcting for the influence of the Fraunhofer lines. He found a satisfactory agreement with Chalonge having obtained color temperatures of 7270°K and 5550°K.

At Pic du Midi, Labs (1957) made a new series of measurements of the profile of the continuous spectrum from 0.33 to 0.7 micron and the absolute intensity of 0.5263 micron (Reference 34). On either side of the Balmer limit he finds values for the temperature of 7540° and 6225°K. These results, obtained with a glass to prism double monochromator, rest on the known energy distribution and calibration of a standard carbon arc, having a temperature  $3949^{\circ} \pm 10^{\circ}\text{K}$ ., and on atmospheric extinction measures obtained independently with interference filters.

For a definitive curve, Minnaert adopts 5780°K. for the wavelengths shorter than 0.37 micron and 7150°K. at the longer wavelengths (Reference 32).

Beyond 2.5 microns, very little work has been done. The infrared radiation in the interval 0.8 to 3.5 microns has recently been measured by Jarosevcev (1956) (Reference 33).

Adel (1939) found that observations of the energy distribution profile from 8 to 14 microns, made with a Lampland thermocouple, could be represented by temperatures from 6000° to 7000°K (Reference 13). However, he recognized that, for these temperatures and wavelengths, the shape of the curve is quite insensitive to the temperature. The problem should be attacked by computing the true intensity ratio between the sun and a standard source at each wavelength. Until this is done it seems likely that the best estimate of the course of the curve can be made from astrophysical theory. Because of the great absorption of the H<sup>-</sup> ion free-free transitions occurring in the far infrared, only the outermost boundaries of the sun radiate to space. Boundary temperatures have been variously disputed as being between 3800° and 4500°K. If we adopt 4000°K., we can then expect, by the Rayleigh-Jeans law, that the absolute intensity will be 2/3 of the value that we should have extrapolated from shorter wavelengths using  $T_b = 6000^{\circ}\text{K}$ .

A remarkable extension of the observation of the photospheric solar spectrum to 2.5 millimeters was accomplished in 1952 by Sinton (Reference 30). His detecting equipment consisted of a parabolic searchlight mirror used to focus the energy passing through a black paper

filter onto a Golay infrared detector. The transparency of the 0.9 to 2 millimeter window is far from complete and, as yet, no absolute values of the spectral energy distribution in this region are available.

The rocket ultraviolet region of the spectrum was first observed in October, 1956, by Baum et al, from altitudes of 88 kilometers. The structure of the energy distribution in the ultraviolet region is determined entirely by the great concentration of the Fraunhofer lines. Few unaffected regions (or windows) exist. Two windows, 0.2977 micron and 0.2913 micron, appear to be nearly free of absorption when observed with a resolution of 0.3 Angstroms. A comparison of the computed radiation through four such windows with the rocket observations is made in the following table. The effective temperature chosen was 6000°K.

<u>Wavelength</u>	<u>J (Observed)</u>	<u>J (Calculated 6000°K.)</u>
0.2977	11.6	9.70
0.2913	10.4	9.04
0.2758	4.7	7.48
0.2700	5.2	6.91

The J's are given in microwatts/cm<sup>2</sup>/A.

In view of the higher radiation in the supposedly clear windows, a radiation temperature of higher than 6000°K might be required.

A spectrogram taken in 1955 from an Aerobee rocket by Johnson et al. shows the solar spectrum from 0.0977 to 0.1817 micron. On this spectrogram, the continuum extends to about 0.1550 micron with Fraunhofer

structure visible to about 0.1680 micron. The energy distribution is very uneven.

Measurement of the energy distribution of the solar radio emission is a recent addition to the astrophysical study of radiation. The sun is the only individual star to be identified as a radio source. Thus, all the known stellar radio radiation data comes from the sun.

The behavior of the sun at radio frequencies is in strong contrast to its behavior in visual radiation. Occasionally the entire observable radio spectrum is involved in violent noise storms, resulting in a vast enhancement of the radio emission. At other times, the sun is quite undisturbed and the radio emission from a so-called "quiet sun" can be studied. At these times it is found that only the radio radiation of wavelengths shorter than about 3 centimeters comes mainly from the region of the solar atmosphere where the optical radiations arise. The radio frequency index of refraction of the solar corona and chromosphere is such that radio waves of longer wavelength must arise in higher and higher elevations above the surface. In fact, the radiation temperature of the disc center has been measured at various wavelengths from 4mm upward. At 4mm the temperature is about 6000° or 7000°K., the temperature of the lower chromosphere, but, as the wavelength of observation increases, the temperature rises until at meter wavelengths the radiation temperature is of the order of  $10^6$  degrees Kelvin, that of the corona.

The general conclusions, then, would seem to be that the sun does not radiate as a perfect black body, but that, in the region between 0.60 micron and the very short radio wavelengths (<3 cm.), a black body distribution of radiation temperature, 6000°K., may be closely approximated. Extension of this conclusion to stars of later spectral type may or may not be justified, but it would seem unlikely that there is a drastic departure from the characteristics of the solar case.

## V. TARGET AND STELLAR INFRARED IRRADIANCE

In the previous semi-annual report, a number of expressions were derived for stellar irradiance and limiting visual magnitude in order to describe the stellar background in various wavelength intervals. It should also be noted that the Johnson-Morgan system of photometry was adopted for the purpose of defining apparent visual magnitudes. By definition, any star of unit-apparent visual magnitude, regardless of spectral type, will produce the same irradiance,  $H_{v1}$ , in the visual band,  $\Delta\lambda_v$ ,

$$\text{where } H_{v1} = 1.5 \times 10^{-13} \text{ watts/cm}^2 \quad (1)$$

and the irradiance of a first magnitude star of spectral class 5, in any wavelength band,  $\Delta\lambda_x$ , is given by

$$H_{x1}(S) = \frac{F_x(S)}{F_v(S)} H_{v1} \quad (2)$$

where  $F_x(S)$  is the fraction of the irradiance in  $\Delta\lambda_x$  and  $F_v(S)$  is the irradiance in  $\Delta\lambda_v$ .

The limiting background stellar irradiance  $H_{xL}$  in  $\Delta\lambda_x$  can be determined from the desired target to background contrast, and the limiting visual magnitude  $m_{vL}$  for each spectral class, which will just yield  $H_{xL}$ , can be found from  $m_{vL}(S) = 1 - 2.5 \log_{10} \frac{H_{xL}}{H_{x1}(S)}$  (3)

For a given target-sensor configuration, equation (3) can be used to define the limits of the stellar background.

For targets that may radiate as black or gray bodies with Planckian energy distribution, the total irradiance  $H_t$  at the aperture of a detecting system over a free space path is given by

$$H_t = \frac{W A_p}{\pi D^2} \text{ watts cm}^{-2} \text{ micron}^{-1} \quad (4)$$

where  $W$  is the total radiant emittance and  $A_p$  is the target projected area at distance  $D$ .

In the presence of an atmosphere,

$$H(\lambda_2 - \lambda_1) = \frac{A_p}{\pi D^2} \int_{\lambda_1}^{\lambda_2} W_\lambda t_\lambda d\lambda \quad (5)$$

where  $t_\lambda$  is the spectral transmittance of the atmosphere.

Irradiance values have been computed in a similar study for a 300°K target of 0.5 emissivity and projected areas of 10 and 2 square meters as a function of range and wavelength interval. Refer to Figure 1. The wavelength intervals selected were 8-13 microns, 3.2-4.2 microns, and 1.5-2.5 microns which coincide with major atmospheric windows. It will be noted that there is a difference of some four hundred times in the effective irradiance over this range of infrared wavelengths.

The standard target conditions for this study follow:

Range	-	500 nautical miles
Skin Temperature	-	300°Kelvin
Projected Area	-	2 square meters
Emissivity	-	0.5

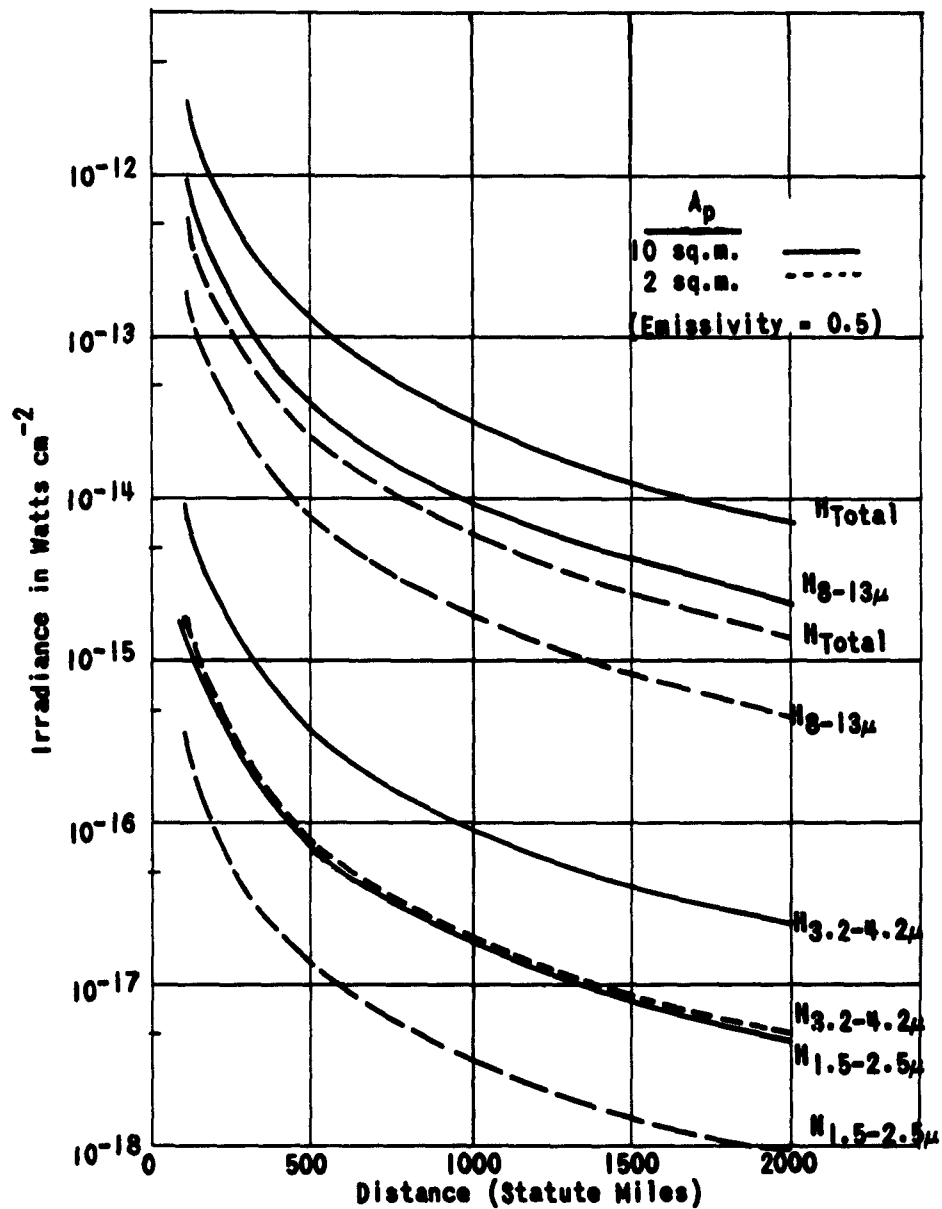


Figure 1. IRRADIANCES OF 300°K SATELLITES IN FREE SPACE AND IRRADIANCES LIMITED BY THE TRANSMITTANCE OF ONE AIR MASS

and the wavelength regions based on selective high sensitivity photoconductive detectors are:

$\Delta\lambda$ 3-4 microns	$\Delta\lambda$ 3-5.5 microns
$\Delta\lambda$ 8-13 microns	$\Delta\lambda$ 8-40 microns

The total irradiance ( $H_t$ ) of the standard target is  $1.7 \times 10^{-14}$  watts/cm<sup>2</sup> and, where the target to background contrast is taken as 10:1, the limiting irradiance in each of the four wavebands is

$H_{3-4}$ microns	-	0.0013	$H_t$	-	$2.2 \times 10^{-18}$	watts/cm <sup>2</sup>
$H_{3-5.5}$ microns	-	0.0023	$H_t$	-	$3.9 \times 10^{-17}$	watts/cm <sup>2</sup>
$H_{7.5-13.5}$ microns	-	0.033	$H_t$	-	$5.6 \times 10^{-16}$	watts/cm <sup>2</sup>
$H_{8-40}$ microns	-	0.080	$H_t$	-	$1.36 \times 10^{-15}$	watts/cm <sup>2</sup>

If it is tacitly assumed that these irradiances are detectable, the limiting stellar visual magnitudes can be calculated for each spectral class from Equation (3). These results are plotted in Figure 2. The desirability of using the longer wavelength bands to minimize stellar background is immediately apparent. In the region beyond 8 microns, none of the blue giants or supergiants appears and cool red stars are evident only down to about 9th magnitude. Furthermore, since the hot blue stars are found primarily in the plane of our galaxy, when these stars are filtered out, the distribution of stars on the celestial sphere becomes more nearly random. This in itself should simplify the additional discrimination required to remove the contributions of the remaining stars.

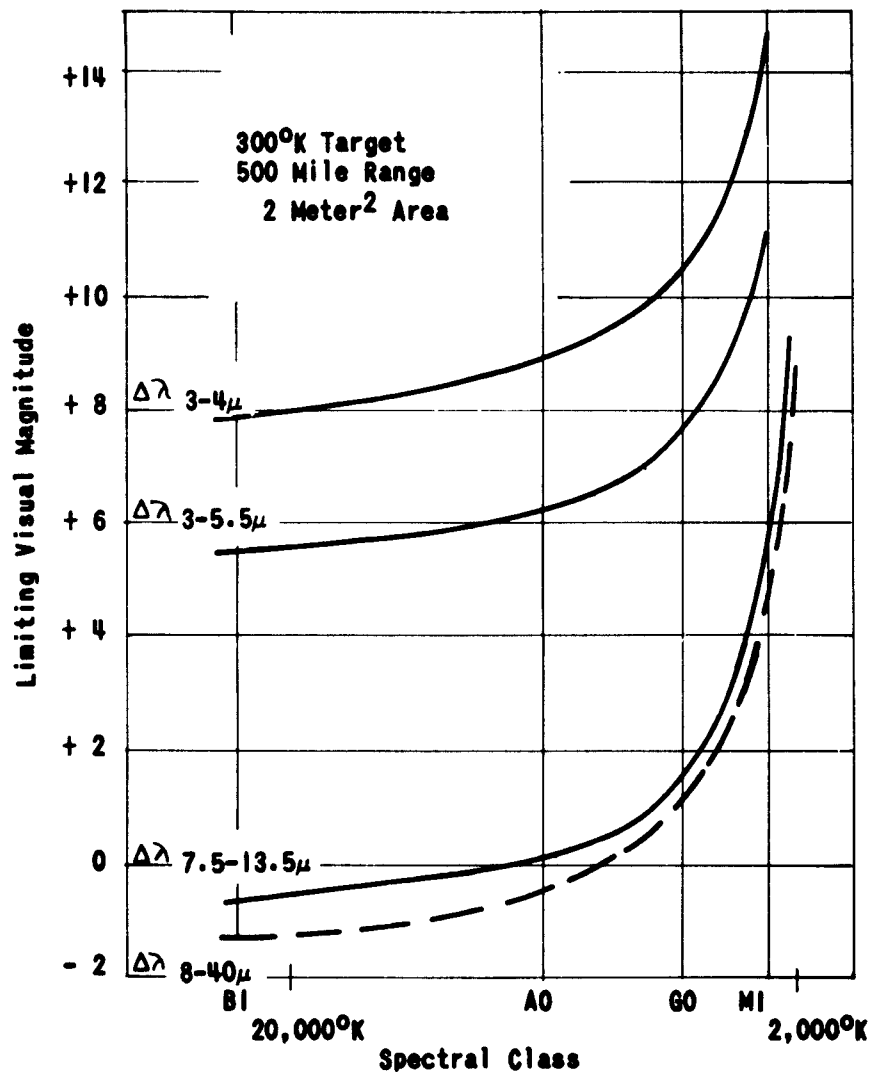


Figure 2. LIMITING VISUAL MAGNITUDE  
FOR STARS  $\frac{1}{10}$  TARGET INTENSITY

It cannot be overemphasized that these predictions of the characteristics of the stellar background at long wavelengths are based upon a relatively narrow wavelength band centered in the visible. There are no measurement data in the 8-13 micron region to substantiate these extrapolations and they must, therefore, be treated as only an estimate of the stellar background in this wavelength region.

## VI. THE INFRARED STELLAR BACKGROUND AND A SYSTEM OF INFRARED MAGNITUDES

### A. AN INFRARED MAGNITUDE SYSTEM

The apparent magnitude of a star in the 7.5 to 13.5 micron region is determined from the computation of the color index, assuming black body radiation, and the apparent visual magnitude of the star. The color index is defined in a similar manner to the color indices used in the conventional magnitude systems of astronomy. We have designated the color index associated with the 7.5 to 13.5 micron region as ZI, given by:

$$ZI = m_v - m_z$$

The zero point of the  $m_z$  scale is given by the condition that  $ZI(AO) = 0.0$ , or that the apparent z-magnitude is equal to the apparent visual magnitude for an AO dwarf star (See Appendix A).

### B. DETERMINATION OF THE Z-INDEX

The values of ZI as a function of spectral type, or of temperature, may be determined easily from the data of limiting visual magnitudes as a function of temperatures for a given infrared irradiance, limiting or otherwise.

Given two stars of spectral type AO and XY respectively:

$$m_v(AO) - m_z(AO) = 0.0 \quad (1)$$

$$m_v(XY) - m_z(XY) = ZI \quad (2)$$

Subtracting (1) from (2):

$$m_v(XY) - m_v(AO) + m_z(AO) - m_z(XY) = ZI \quad (3)$$

If the two stars have the same irradiance in  $\Delta\lambda_z$ , their z-magnitudes will be equal:

$$m_z(AO) = m_z(XY) \quad (4)$$

so that for a given irradiance in the 7.5 to 13.5 micron range, or for a given apparent z-magnitude, the color index ZI can be obtained by equation 5, (obtained by substitution of equation 4 into 3).

$$m_v(XY) - m_v(AO) = ZI \quad (5)$$

From equation 5, it can be stated that the z-index can be determined as a function of spectral type (XY), by simply subtracting from the limiting visual magnitude of the star by spectral type (XY) the limiting visual magnitude of the star of spectral type (AO) providing the limiting magnitudes have been computed for the same limiting irradiance.

#### C. LIMITING MAGNITUDE

In order to keep the number of stars under investigation within reasonable bounds it becomes necessary to limit the brightness of stars to be considered. Various factors affect the choice of magnitude limits in this study.

If one is going to consider all stars in the sky brighter than a certain limiting brightness, the numbers become large quite rapidly.

The number of stars brighter than a given apparent visual magnitude distributed all over the sky are listed in Table I.

TABLE I

<u>Visual Magnitude Limit</u>	<u>Number of Stars</u>
1.0	12
2.0	41
3.0	141
4.0	543
5.0	1620
6.0	4850
7.0	14300
8.0	41000
9.0	117000

It is apparent that to treat the whole sky one must set a limit which will produce a usable number of stars. As a start it was decided that magnitude scales be set up for all stars brighter than visual magnitude +3.0 to see how effective the spectral discrimination would be to this limiting magnitude. The magnitude limit was later extended to apparent visual magnitude +6.0 to provide information on most of the stars contained by the limiting magnitude curve of Figure 2 for  $\Delta\lambda$  7.5-13.5 microns ( $m_z \leq 0.0$ ). From the nearly 5000 stars thus considered, a list was compiled of the 186 stars brighter than the z- limiting magnitude in the 7.5 to 13.5 micron region.

This compilation was greatly simplified because many of the earlier spectral types could be eliminated immediately because their visual magnitudes are fainter than the limiting visual magnitude for their spectral

type. Table II lists the magnitude limits for each spectral type and luminosity class used in this survey.

TABLE II  
LIMITING APPARENT VISUAL MAGNITUDE  
FOR STARS HAVING  $m_z = 0.0$

Spectral Type	Luminosity Class			
	V	VI	III	I-II
O	-0.2			
B	-0.1			
A	+0.7			+1.0
F	+1.5	+1.7	+1.8	+2.1
G	+2.1	+2.6	+3.1	+3.6
K	+3.7	+3.9	+4.6	+4.9
M	+6.0	+6.0	+6.0	+6.0

D. STELLAR DATA

Spectral types for the stars were taken from the Mount Wilson Catalogue of Radial Velocities. These are considered to be the most accurate spectral classifications available for a large number of stars. The Catalogue lists stars fainter than  $m_v = 6.0$  but may not be quite complete to the 6th magnitude. Thus the list of stars observable in the 7.5 to 13.5 micron region is probably complete in the range  $-6.0 < m_z < -1.0$  but not quite complete in the range  $-1.0 < m_z < 0.0$ . A few stars fainter than  $m_v = +6.0$  which would have  $ZI > 6.0$  magnitudes were not included because of the uncertainty of the completeness of the Catalogue at fainter magnitudes. These stars, at any rate, would fall in the range  $-1.0 < m_z < 0.0$ .

The spectral Type-Temperature calibration was taken from the Morgan-Keenan article in "Astrophysics" edited by Hynek. Some interpolation was necessary but it is felt that this had little effect upon the results. However, some rather extensive extrapolations became necessary and the results in these cases may be off by as much as one magnitude.

The color indices are determined as a function of temperature and then expressed in terms of spectral type. These data are tabulated in Appendix A.

#### E. DISCUSSION OF THE INFRARED PLOTS

The 186 stars brighter than 1/10 target intensity, to  $m_v = +6.0$ , are listed in Appendix B. Included in this table, following a catalogue number, are the 1950 positions, spectral type, apparent visual magnitude, z- color index, apparent z- magnitude, and the star designation, which consists of the Mount Wilson Radial Velocity Catalogue number and the Bayer or Variable star designation.

The Plumbide Index (3.0-4.0 microns) and apparent magnitude are not included in this table. The color indices are not substantially different from the z- indices and the apparent magnitudes in the 3.0 to 4.0 micron region for the listed stars are thus about the same as the z- magnitudes. The only difference between the two regions is the limiting magnitude. The 3.0 to 4.0 micron limiting magnitude is about 2.5 magnitudes fainter than the z- region, which means there would be about 2000 stars to consider instead of 185.

Figure 3 is a plot of the entire sky showing only stars to apparent visual magnitude, +3.0. The tendency to concentrate to the plane of the galaxy is evident. The galactic plane is roughly located in a circle centered just below the center of the plot.

Figure 4 is a plot of the same stars as Figure 3 which are also detectable by means of the z- detector,  $m_z = 0.0$  or brighter.

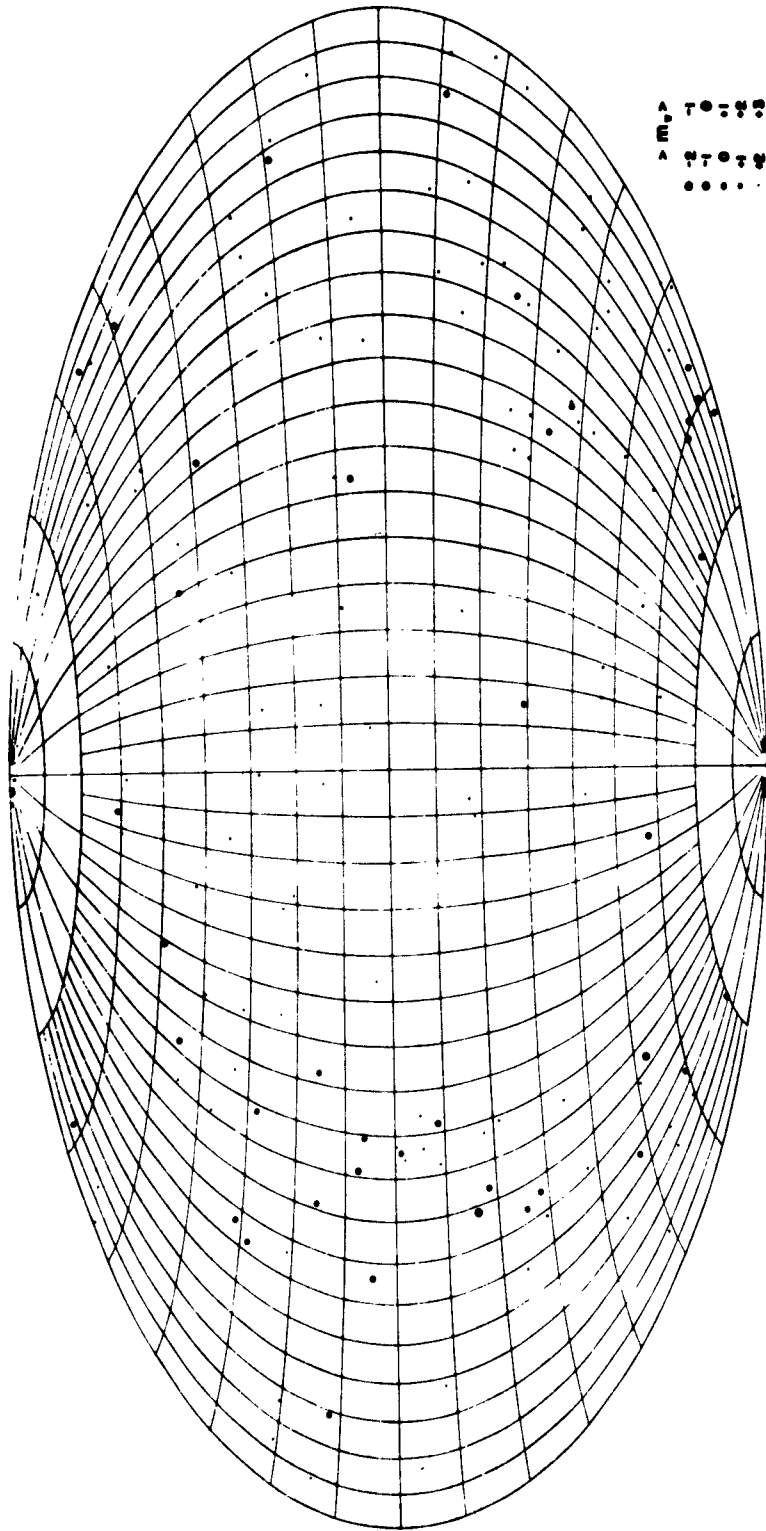
Figure 5 is a plot of all 186 stars brighter than  $m_v = +6.0$  and  $m_z = +0.0$ .

Figure 6 is a plot of all stars brighter than  $m_v = +6.5$  in the region of the sky  $1^h40^m < \alpha < 6^h20^m$ , and  $+60^\circ > \delta > -60^\circ$ .

Figure 7 is the same region of the sky as Figure 6 with only those stars brighter than  $m_z = 0.0$  plotted.

The first notable feature of these plots is the great decrease in numbers of stars when one observes at the long wavelengths. This immediately suggests the power of spectral discrimination when using a detector in the 7.5 to 13.5 micron region at the present limiting magnitudes.

A second feature is the tendency for the infrared objects to become a little more randomly distributed, showing less concentration to the galactic plane. Whether this tendency will continue to fainter limiting magnitudes is a matter to be answered by observation.



**Figure 3. ALL STARS BRIGHTER THAN APPARENT VISUAL MAGNITUDE  
+3.0 PLOTTED ON AN EQUAL AREA PROJECTION  
OF THE ENTIRE SKY**

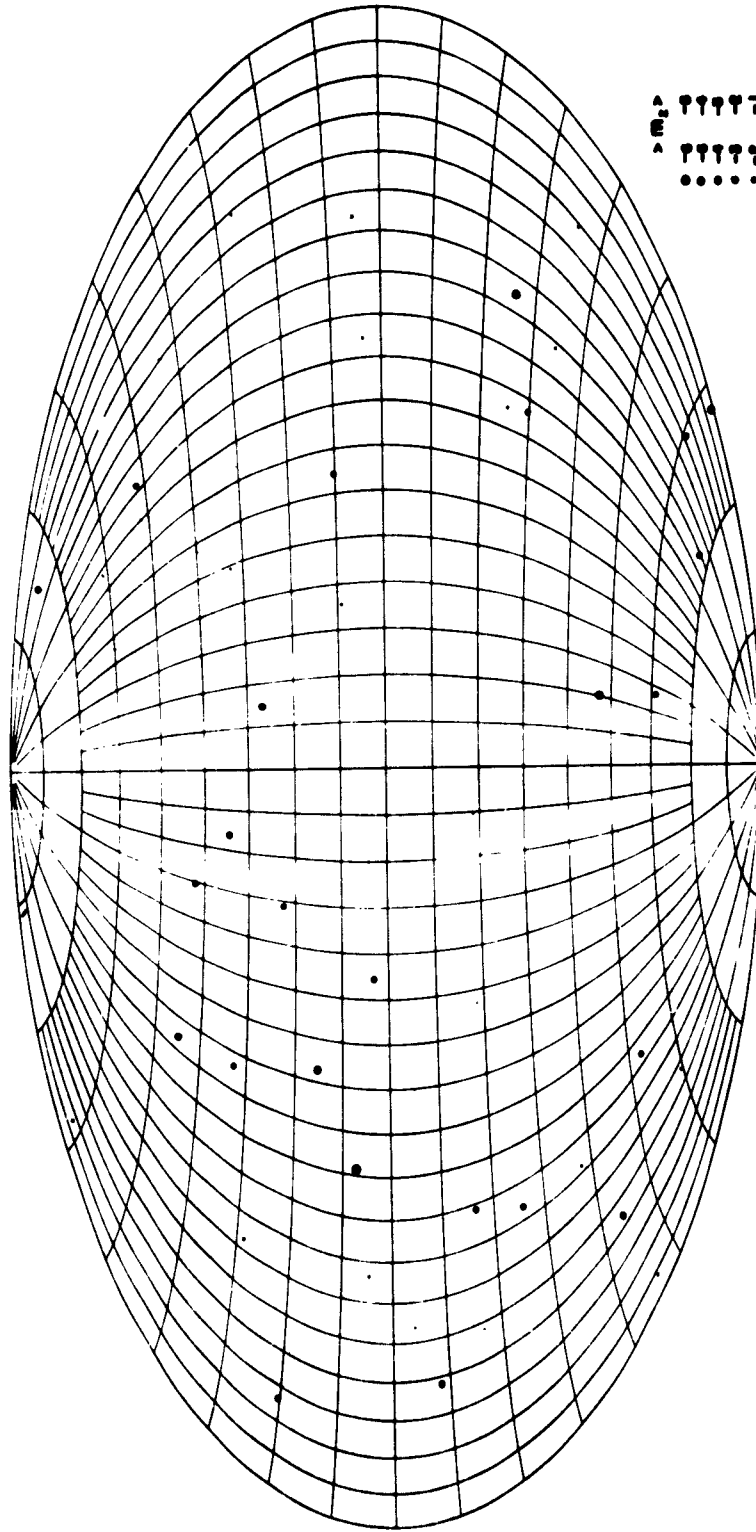
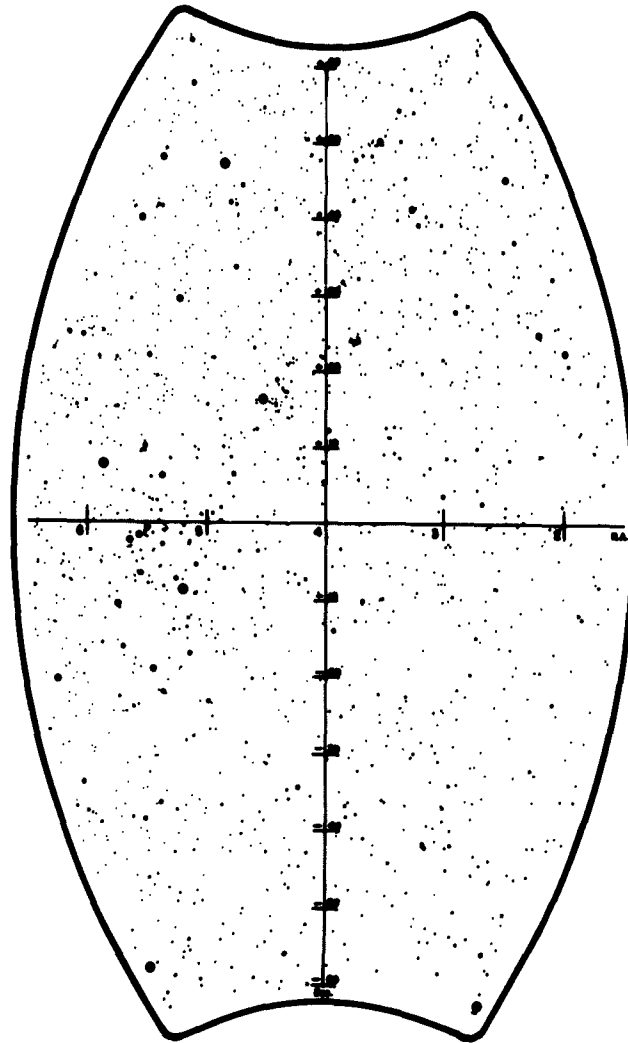


Figure 4. ALL STARS BRIGHTER THAN APPARENT VISUAL MAGNITUDE +3.0 AND BRIGHTER THAN APPARENT Z-MAGNITUDE 0.0





**Figure 6. ALL STARS BRIGHTER THAN APPARENT VISUAL MAGNITUDE  
+6.5 IN THE REGION OF THE SKY BETWEEN RIGHT ASCENSION  
1<sup>h</sup> 40<sup>m</sup> AND 6<sup>h</sup> 20<sup>m</sup>, AND DECLINATIONS  $\pm 60^\circ$**



The distribution of the observable z- stars with  $m_z$  is as follows:

Magnitude Interval $\Delta_{mz}$	Number of Stars
-6.0 to -5.0	1
-5.0 to -4.0	5
-4.0 to -3.0	14
-3.0 to -2.0	19
-2.0 to -1.0	39
-1.0 to -0.0	<u>123</u>
Total	185

Thus an increase in sensitivity of a factor of 10 will increase the number of stars in the list to about 2500. It is not possible to accurately predict the distribution of these stars as there is no source of accurate spectral types for stars fainter than  $m_v = +7.0$ . The Henry Draper Catalogue, which contains the magnitudes and spectral types of 225,000 stars, is not detailed sufficiently in the classification of later spectral types (i.e., cooler stars) to obtain adequate temperatures for computing color indices in the z- region.

It would seem that, on the basis of the data assembled, a combination of spectral and position or motion discrimination techniques might provide a solution to the problem. The numbers of stars involved at the present sensitivity would not rule out the possibility of programming the positions and brightnesses of the known stellar infrared emitters into a storage drum, the contents of which could then be compared with the output display of an infrared seeker.

## VII. A PROGRAM FOR INFRARED ASTRONOMICAL PHOTOMETRY

### A. OBSERVING PROGRAM

It is planned to initiate a program of infrared stellar photometry to provide a description of the space background on a more sound basis. The projected series of observations of astronomical sources at infrared wavelengths will consider:

1. The known sources approximately in the order of their brightness for those sources not already well measured.
2. The unknown sources approximately in the order of their likelihood to be observed.

The astronomical sources are described further as follows:

1. (a) The bright stars which have thus far been the chief interest in the theoretical work on the stellar background - for the purpose of testing the simple theory that the normal stars radiate at longer infrared wavelengths, as they would if they were black bodies at temperatures deduced from their radiations in the visual region of the spectrum.
- (b) A small number of peculiar stars whose composite spectra suggest that the systems have a large infrared component.
- (c) The region of the Galactic nucleus - because of their greater ability to penetrate dust and gas, the longer infrared wavelengths will allow a deeper survey of the

highly obscured innermost regions of our Galaxy than is possible at shorter wavelengths. On the other hand, the shortness of these same wavelengths relative to radio wavelengths makes them capable of producing a more detailed picture of the Galactic nucleus.

2. (a) Protostars, as have been suggested from radio observations to exist in the younger galactic clusters and stellar associations.
- (b) Other well known agglomerations of dust and gas, but which lack visible stellar components. These might well be examined for protostars.
- (c) A sky survey in the manner of surveys long ago undertaken at visual wavelengths and, in recent years, at numerous radio wavelengths - the scope and depth of such an infrared survey depends, of course, on what extent a real discrimination can be achieved with some sort of two-dimensional detector array. In its initial phase, this survey should concentrate on the area of the Milky Way.
- (d) Extragalactic Systems - in recent work on nearby elliptical galaxies Kelvin bodies of  $1900^{\circ}$  temperatures have been hypothesized to exist alongside the observable constituents

in order to account for the large reddening observed in these systems at wavelengths less than one micron. The extent of the reddening beyond one micron is at present, however, unknown.

#### B. INSTRUMENTATION

Initially, a simple infrared photometer using the best available uncooled detectors will be used with the Ohio State 69-inch Perkins reflector. This instrument has been designed and constructed and is presently in use at the observatory. A view of the elements of the optical system is shown in Figure 8. Three detectors are available for measuring stellar radiation in different infrared wavebands. They are a lead sulfide cell with a filter for 2.0-2.4 microns, lead selenide with filter for 3.5-4.0 microns and a thermocouple with filter for 7.5-13.5 microns. These detectors may be alternately switched into a low-noise variable bandwidth electronic system followed by a recorder.

Computations have been made based on the noise equivalent power of the detectors within the wavebands of interest in order to determine the limiting visual stellar magnitudes for the 69-inch Perkins reflector. Figure 9 presents this data for a system bandwidth of one cycle/second, a signal to noise of one, and an assumed optical transmittances of 0.5. Under these conditions only several stars will be detectable with the bolometer detector in the 7.5 to 13.5 micron region. To improve this situation, very

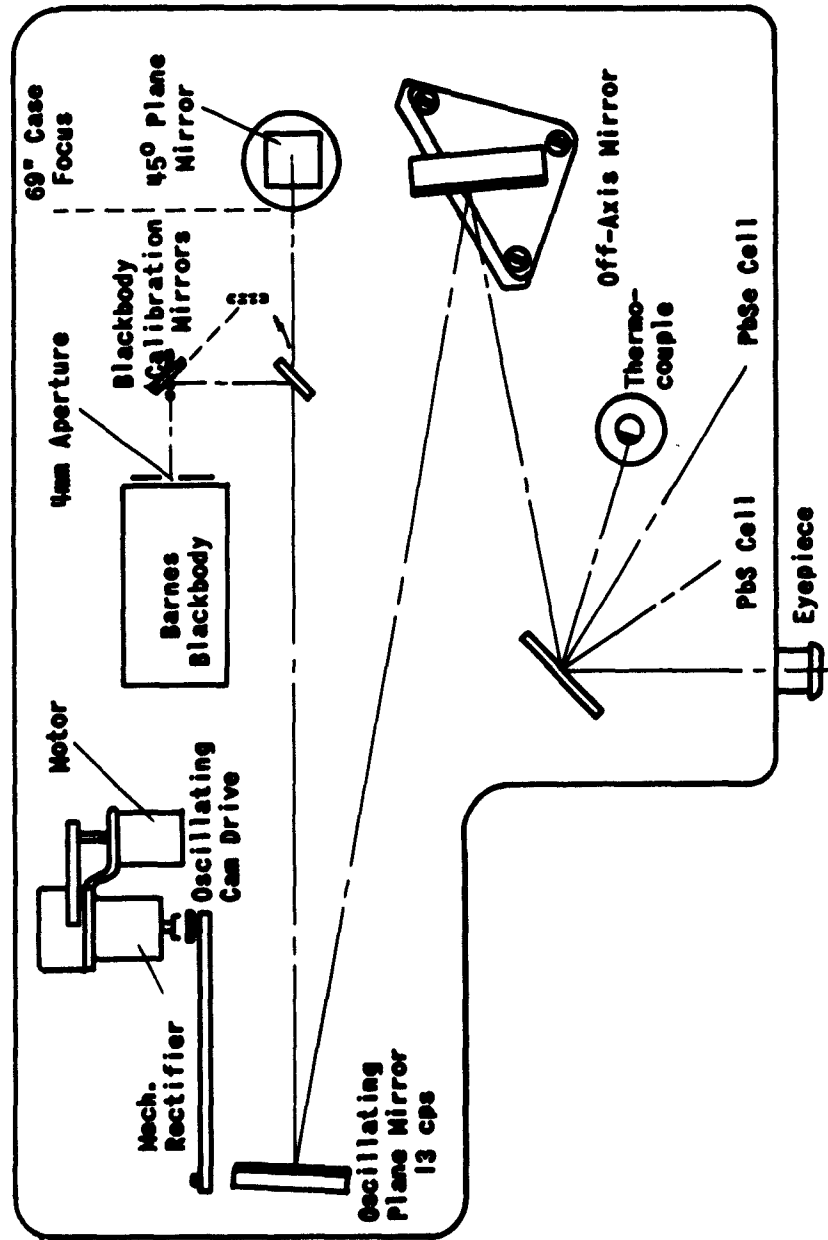


Figure 8. IR STELLAR PHOTOMETER OPTICAL SYSTEM

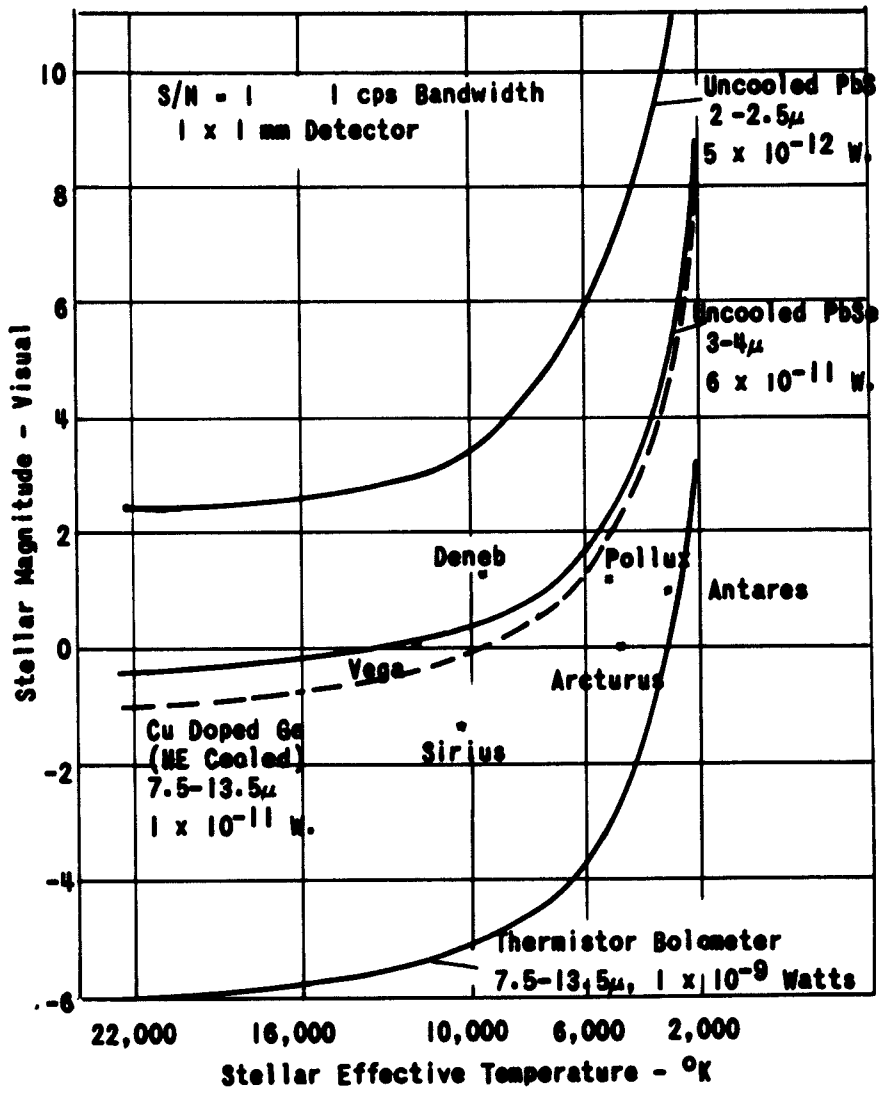


Figure 9. LIMITING STELLAR MAGNITUDES FOR VARIOUS INFRARED DETECTORS AND THE 60-INCH PERKINS REFLECTOR

narrow bandwidths on the order of .01 cycle/second will be employed. The next step in improving the long wavelength photometer performance will be the substitution of a helium cooled doped germanium detector such as the Cu:Ge detector noted in the figure. This detector will permit observation of about the same number of stars as can be observed in the 3 to 4 micron region with uncooled lead selenide.

The use of relatively broad band multilayer interference type filters, paired to appropriate detectors, is considered essential to this task. These filters are a recent development which have the desirable characteristics of relatively sharp spectral cuts, good transmission in the passband, and a high degree of sideband suppression. They are quite complex in many instances, requiring as many as eleven or more alternating high and low-index layers deposited with a high degree of thickness and uniformity. The spectral transmittance of two of these filters in the 2.0 to 2.4 micron and 8.0 to 13.0 micron region are shown in Figures 10 and 11 respectively.

In carrying out a program of infrared photometry as is proposed, it is necessary to know very closely the spectral response ( $S\lambda$ ) of the detector in question, the atmospheric spectral transmittance ( $T\lambda$ ), the filter spectral transmittance ( $t\lambda$ ), and the spectral distribution of black-body energy ( $H\lambda$ ) at a particular temperature. Product curves of these variables may be plotted as shown in Figures 12, 13, 14 and 15 for 2000°K and 6000°K black body emitters against lead sulfide and thermocouple

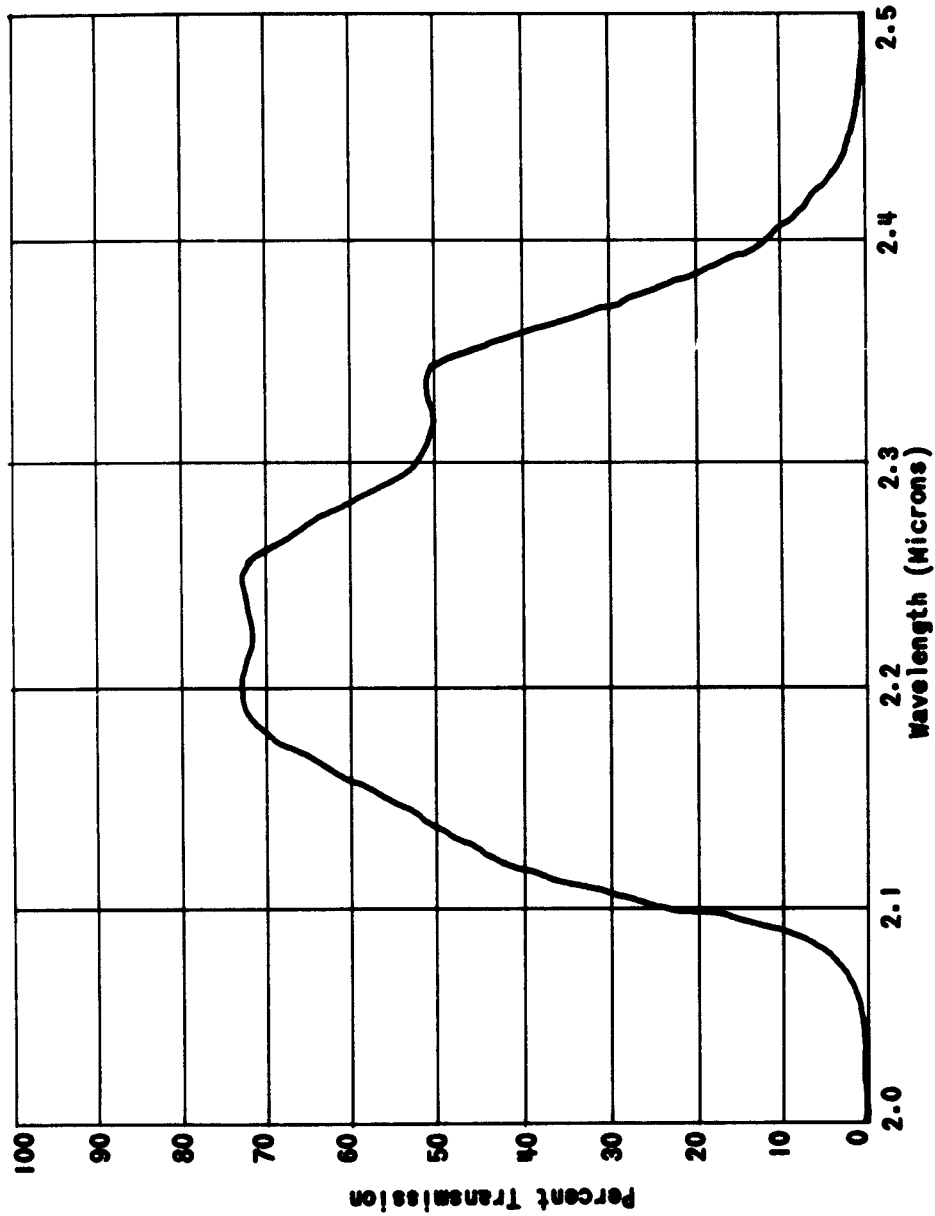


Figure 10. SPECTRAL TRANSMITTANCE OF A 2.0-2.4 MICRON MULTI-LAYER INTERFERENCE FILTER

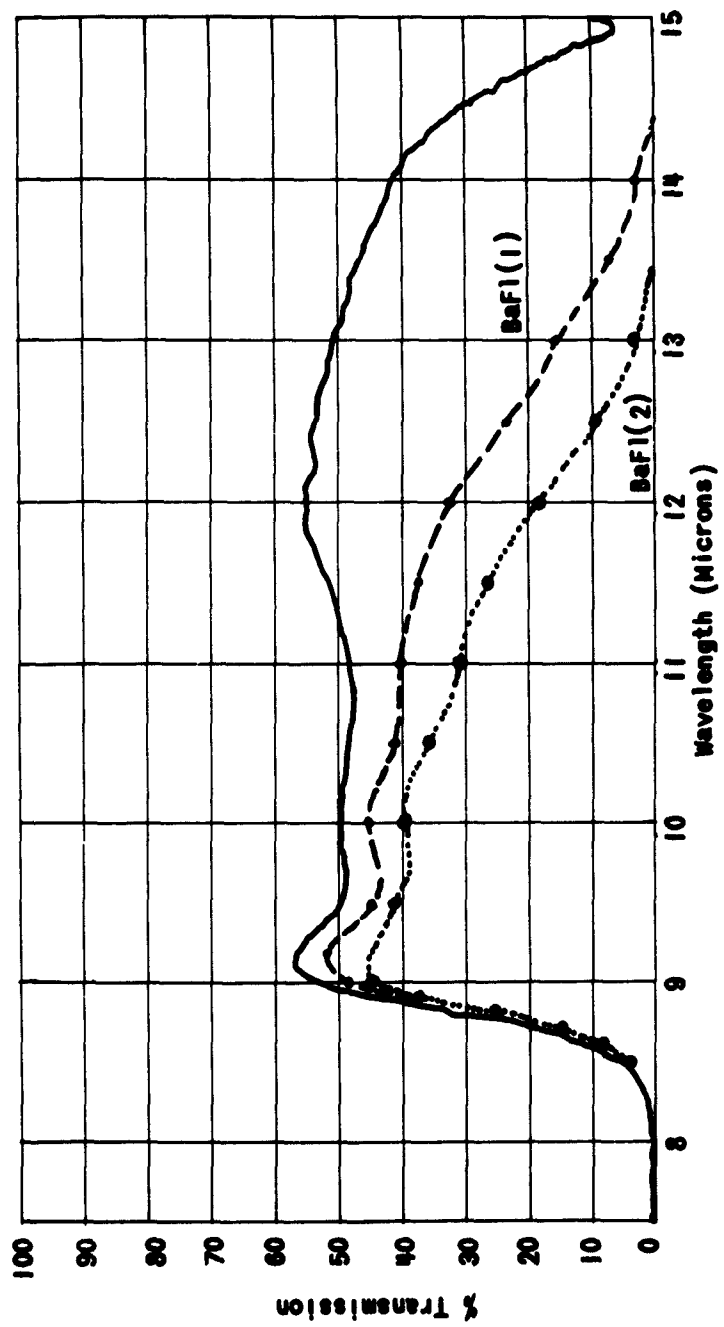


Figure 11. SPECTRAL TRANSMITTANCE OF A 8.0-13.0 MICRON MULTILAYER INTERFERENCE FILTER IN COMBINATION WITH BARIUM FLUORIDE WINDOWS

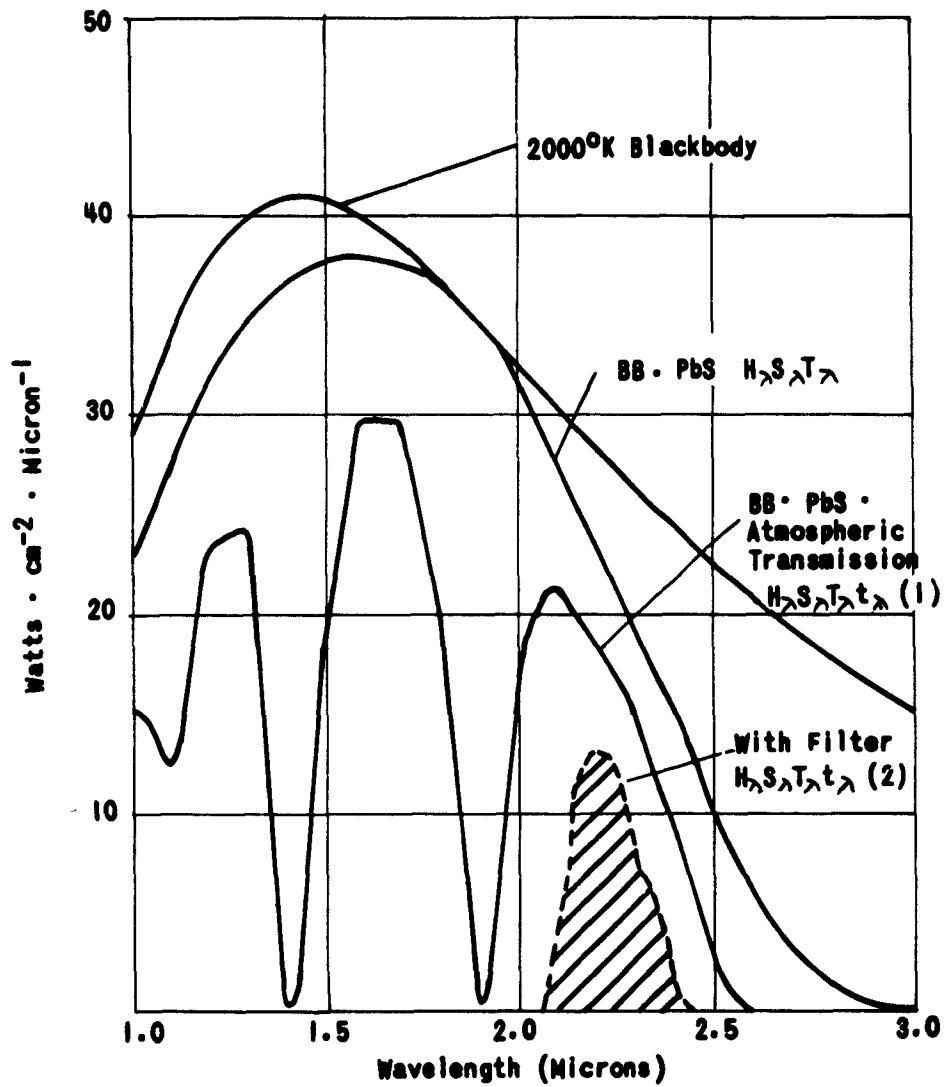


Figure 12. PRODUCT CURVES FOR A 2000°K BLACKBODY IN THE LEAD SULFIDE 2.0-2.4 MICRON REGION INCLUDING THE EFFECT OF ATMOSPHERICS

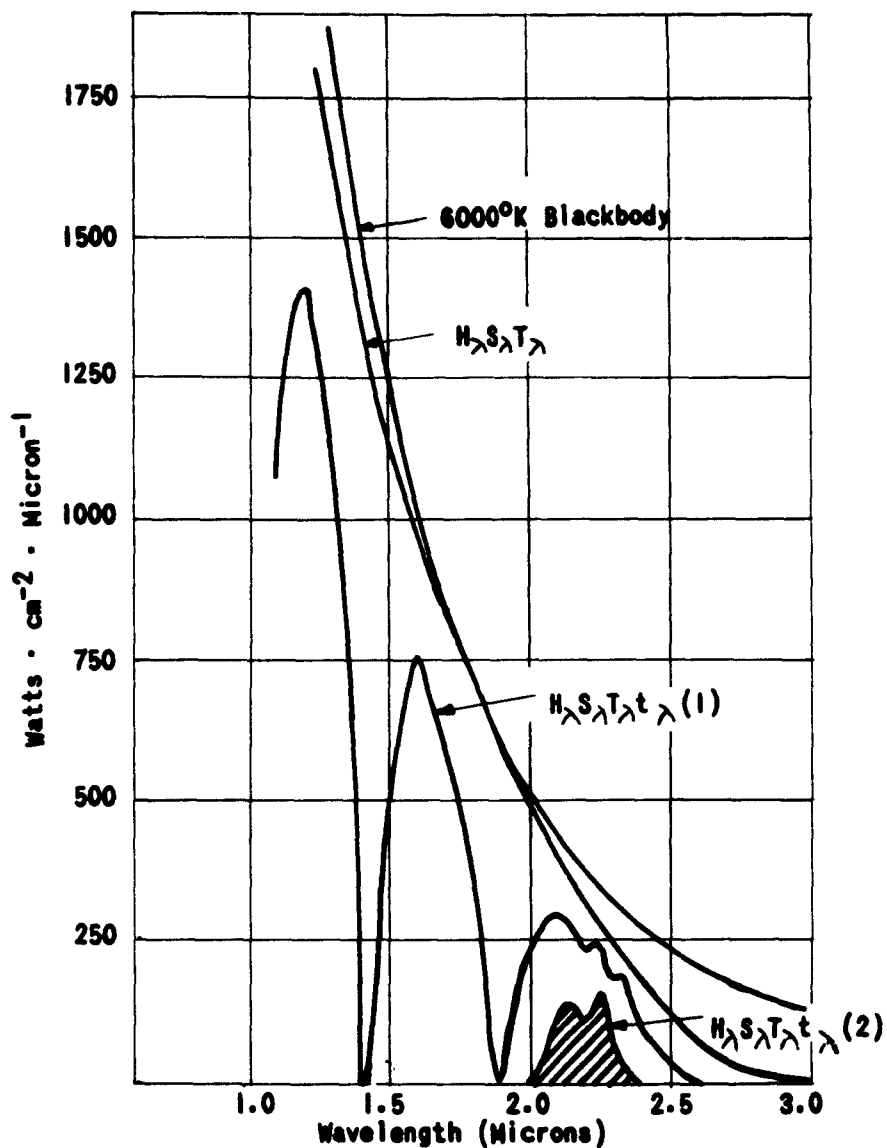


Figure 13. PRODUCT CURVES FOR 6000°K BLACKBODY IN THE LEAD SULFIDE 2.0 TO 2.4 MICRON REGION INCLUDING THE EFFECT OF ATMOSPHERICS

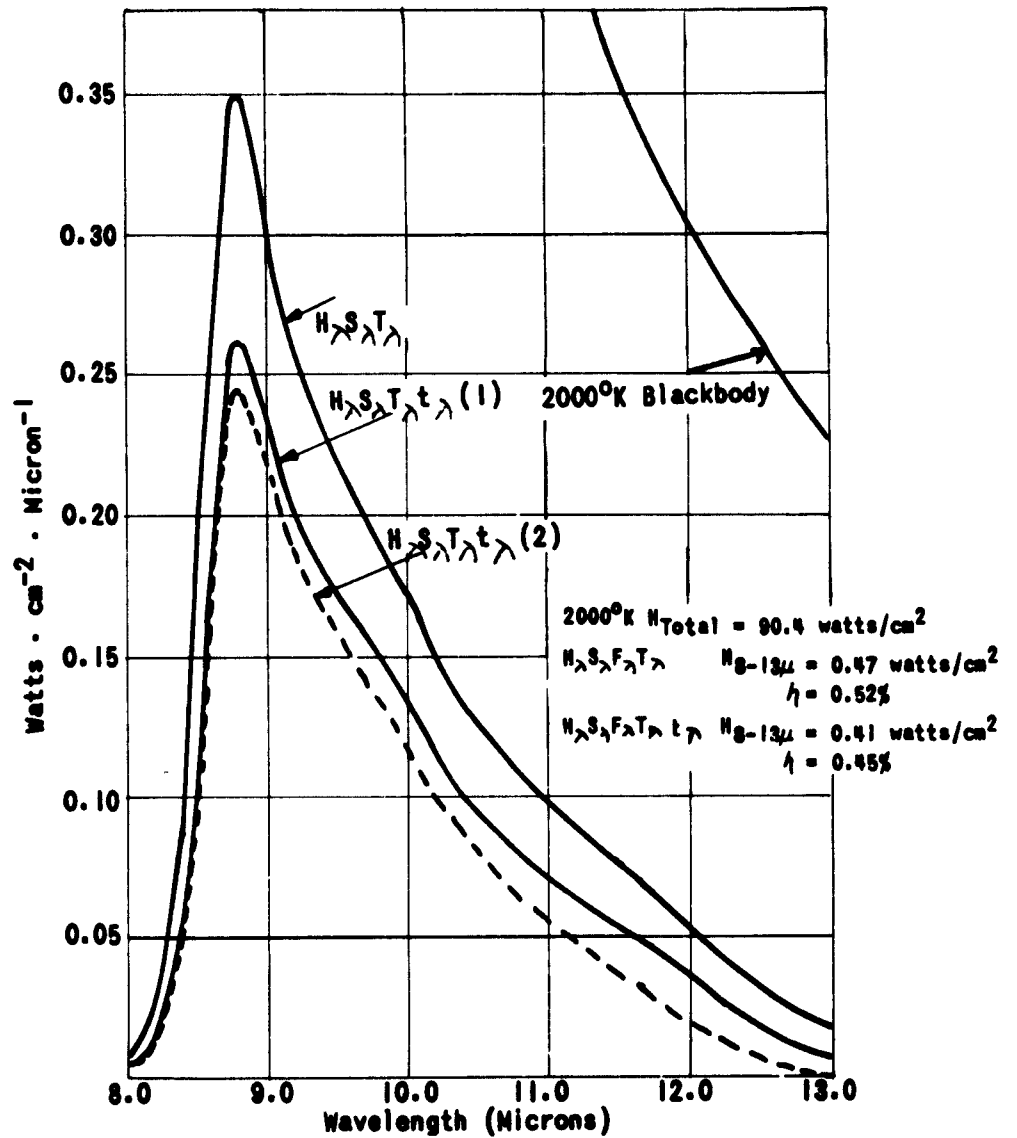


Figure 14. PRODUCT CURVES FOR 2000°K BLACKBODY IN THE THERMOCOUPLE 8-13 MICRON REGION INCLUDING THE EFFECT OF ATMOSPHERICS

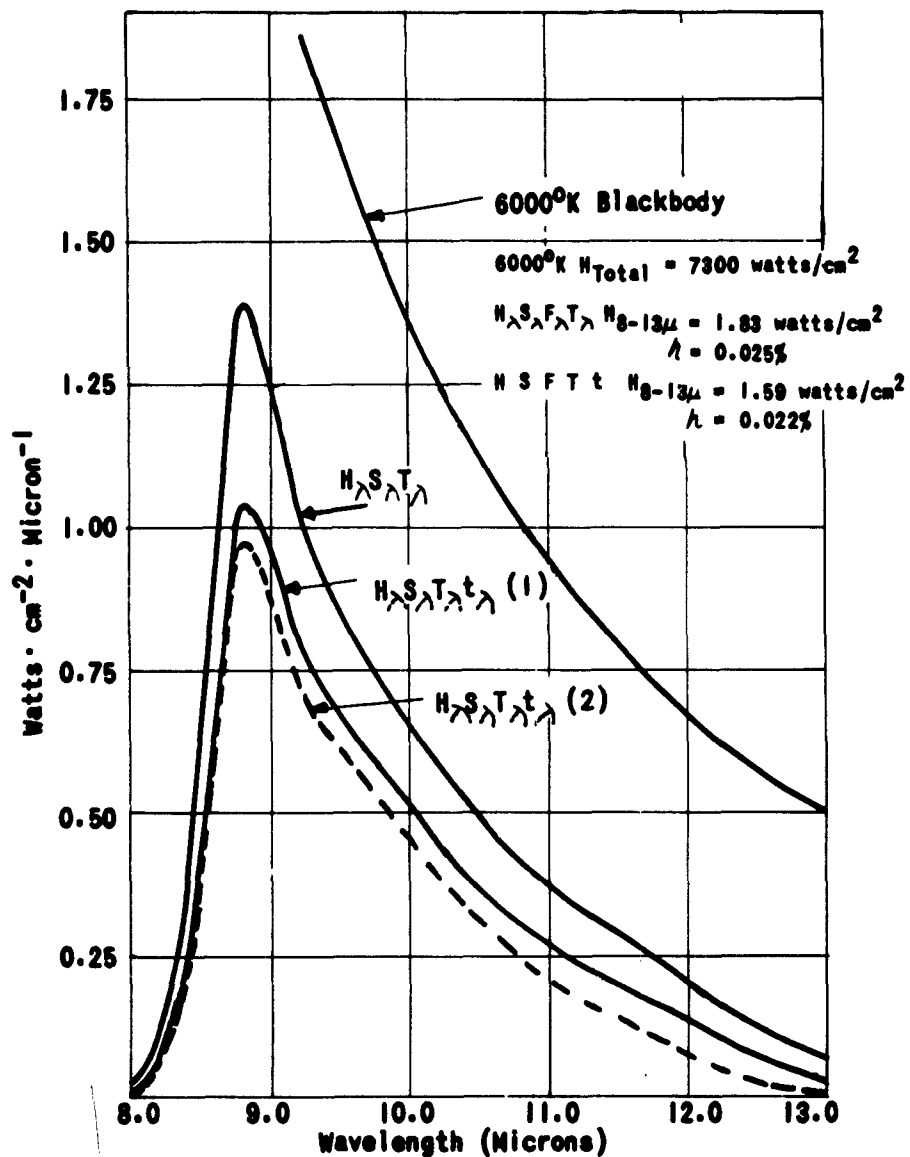


Figure 15. PRODUCT CURVES FOR  $6000^{\circ}\text{K}$  BLACKBODY IN THE THERMOCOUPLE 8 TO 13 MICRON REGION INCLUDING THE EFFECT OF ATMOSPHERE

detectors. For our system of infrared photometry, interest is obviously centered on the  $H\lambda S\lambda T\lambda t\lambda$  curves which may be integrated mechanically to obtain effective irradiance. A family of similar curves has been plotted for stellar classes B through M and temperatures from 22,500° to 2000°K.

C. POSSIBLE INFRARED EMITTERS THAT ARE NOT NORMAL STARS

Assuming that the blackbody calculations provide the known stellar objects which are observable in the 8 to 13 micron region, the question then arises as to the objects which are not typically stellar in nature, or the unusual objects which cannot be classed as normal stars. Is there reason to believe that there are objects which might emit sufficient infrared radiation to provide additional problems in the spectral discrimination techniques?

Such objects will be considered briefly in two categories:

1. Stellar or star-like objects
2. Essentially non-stellar objects; nebulae and/or collections of stars.

D. STELLAR TYPE OBJECTS

Normal stars as well as the so-called peculiar stars most likely will not provide any unusual addition to the infrared background problems.

White dwarfs will not be detectable in the 8 to 13 micron region. Sirius B, which is among the intrinsically brightest white dwarfs lies at a distance of just over 2.7 parsecs and has an apparent z-magnitude

of + 7.8. In order to be detected at the earth, its apparent z-magnitude would have to be brighter than  $m_z = 0.0$  which would be true only if it were at a distance of less than 0.069 parsecs or 0.225 light years. At this distance Sirius B would have an apparent visual magnitude,  $m_v = +0.5$ . So far no white dwarf has been observed brighter than  $m_v = +8.0$ . This seems to effectively eliminate white dwarfs from the background problem.

Very large, tenuous, supergiant stars are known in some eclipsing binary systems. Zeta Aurigae contains a K5 supergiant with a B8 companion. Epsilon Aurigae has been thought for some time to consist of an F supergiant and a large cool mass of gas at a temperature which has been estimated to be as low as  $1100^\circ\text{K}$ . The question arises as to whether there may be even cooler supergiants, which, due to their extreme size and therefore very large surface area, produce a substantial portion of their radiation in the far infrared and still remain sensibly invisible at the shorter wavelengths. A star which seems to be approaching this condition is  $\zeta$  Herculis. An M5 I star, nearly 1000 astronomical units in diameter, it lies at a distance of 500 light years. Its apparent visual magnitude is +3.0. Its apparent z-magnitude is -3.8. This gives an absolute z-magnitude of  $M_z = -9.7$ . A star of this absolute infrared magnitude would be detectable at a distance as great as 800 parsecs or 2500 light years. If even a few such objects exist in a given volume of space they would probably add to the background problem.

It has been suggested that a number of uniformly distributed sources of radio radiation may be due to red dwarf stars. An M5 V star,  $M_V = +10$ , would have an  $M_Z = +4.0$ . This means that to be detectable in the z-region the star must be closer than 1.6 parsecs or about 5 light years. The space density of red dwarfs is relatively high. There are 11 red dwarfs among the 22 stars nearer than 4 parsecs. The limit of about 2 parsecs we have placed upon the distance at which red dwarfs could be observed in the z-region, seems to eliminate them from the possibility of causing any additional background problem. The known red dwarfs within this distance are already on our list.

The existence of protostars or masses of interstellar material contracting under their own gravitational attraction represents a vital step in the present theory of stellar evolution. As these bodies contract, the gravitational energy is utilized in two ways, one-half being radiated away thermally by the contracting mass, the other half going to heat up the matter in the protostar. The existence of such material is strongly suggested by some radio observations and a few of these protostars have been observed in the visual wavelengths before they have reached the main sequence of the Russell Diagram where they begin generating their own thermonuclear energy. It would be worth while to seek infrared sources of this sort in a number of the nearby young, open clusters. Recently F.G. Dyson has proposed a unique type of object which might radiate in the infrared at the total rate of a typical star. (Science, June 1960).

#### E. NON-STELLAR OBJECTS

A strong source of infrared radiation has been recognized and observed for some time. This is the region of the nucleus of the galaxy. This region is populated by a large number of predominately cool stars and the cumulative effect is that of a large surface area source of infrared radiation. Visual radiations are effectively cut off by dust lying between the sun and the nucleus, but infrared and radio waves can penetrate much of the obscuring dust.

The gaseous nebulae shine primarily as a result of hydrogen emission with much of the light being produced in the Balmer Series. However, some radiation may occur in the infrared series, which would make it worth while to observe some H II regions with the IR detectors.

Very dense clouds of dust which can be observed optically only by the fact that they completely cut off the light coming from behind them may be a suitable location for the formation of protostars. They should be investigated to determine the upper limit of their infrared emission.

Some radio sources show steadily increasing flux density with decreasing wavelength. If this trend were to continue down through the microwave region there might possibly be sufficient energy in the infrared to be detected.

There is much interest in the behavior of the spectrum of extragalactic objects. It is just possible that a few of the nearest galaxies might be detectable in the 8 to 14 micron region.

## APPENDIX A

### BANDPASS CHARACTERISTICS OF MAGNITUDE SCALES

Basically, the definition of stellar magnitude scales goes back to the seemingly arbitrary division of the visible stars into six groups by Claudius Ptolemy for the purpose of identification in his catalog of naked-eye stars, "The Almagest."

About 1830, John Herschel concluded that a geometrical progression in the apparent brightness of the stars is associated with the arithmetical progression of their magnitudes. The problem was then to ascertain the ratio of brightness corresponding to a difference of one magnitude, which would best represent the magnitudes already assigned to the naked-eye stars by Ptolemy.

Pogson at Radcliffe in 1856 proposed the adoption of the ratio 2.512 (whose logarithm is 0.4, a convenient value), differing only a little from the average ratio derived from his own observations and those of other astronomers. He adjusted the zero point of this fixed scale so as to secure as good agreement as possible with the early catalog at the sixth magnitude. The scale is now generally accepted.

Pogson's rule is a special case of a general psycho-physical relation established in 1834 by the physiologist Weber, and given a more precise phrasing by Fechner, in 1859. Fechner's law states

$$S = c \log R \quad (1)$$

where  $S$  is the intensity of a sensation

$R$  is the stimulus producing it, and

$c$  is a constant of proportionality.

Pogson had evaluated the constant in the corresponding relation:

$$m - n = c \log(l_n/l_m) \quad (2)$$

where  $l_m$  and  $l_n$  are the apparent brightnesses of two stars whose magnitudes are  $m$  and  $n$  respectively. The constant,  $c$ , is 2.5, or  $1/0.4$ , or  $1/\log 2.512$ .

Thus if the difference,  $m-n$ , is one magnitude,  $\log(l_n/l_m) = 2.512$ .

In general, the ratio of apparent brightness,  $l_n/l_m$ , of two stars whose magnitudes are  $m$  and  $n$ , (or indeed, the ratio of apparent brightness of two regions of the same star's energy distribution for which magnitudes are defined,) can be derived by the formula:

$$\log(l_n/l_m) = 0.4 (m-n) \quad (3)$$

Using, for instance, the photographic apparent magnitude and the visual apparent magnitudes for a given star (which defined the "color index" of the star by the relation:  $C.I. = m_{pg} - m_v$ ), we get the relation between the color index and the ratio of the intensities of radiation in the two spectral regions used to determine the two magnitudes:

$$\log(l_v/l_{pg}) = 0.4 (m_{pg} - m_v) = 0.4 C.I. \quad (4)$$

The color index system has been arbitrarily defined to provide  $C.I. = m_{pg} - m_v = 0$  for AO dwarf stars, the effective temperature  $T_e$  (from  $E = cT_e^4$ ) of which is 11,000°K. Thus, the bandwidth of the photographic region is adjusted to provide, with an 11,000°K energy curve, the same photographic image as the visual region as defined by a filter-plate combination to reproduce the luminous response of the human eye.

The procedure in practice, for determining stellar magnitudes and colors, consists of measuring magnitude and colors against established standards, generally on a magnitude-color system, independent of the fundamental system, yet fully consistent with the fundamental system since all measurements are made relative to each other. The only requirement is that some object of known magnitude and color (fundamental or secondary standard) be observed, along with the unknown stars, so that the observations may be reduced to the fundamental system. The fundamental system used, either the International System or the Johnson-Morgan system, ultimately defines the color index scale by AO stars.

If a photometric system differs much in bandwidth characteristics from the fundamental system, the observed colors will differ considerably from the standard stars. This generally results in non-linear corrections to the observed colors to produce the colors on the fundamental system.

All stellar color systems are based upon magnitude differences involving in some way apparent visual magnitude. Thus, we should start with the fundamental definition of stellar magnitudes, to establish any new magnitude systems. This is the luminous response of the eye, defining the apparent visual magnitude.

Originally magnitudes were of necessity measured visually. Even then, differences in the color response from one observer to the next were noted. Difficulties were encountered then in placing visual magnitudes on a rigorous scale, such as the Pogson scale. The zero point of any magnitude scale must then be defined as some agreement concerning the mean magnitude of certain standard stars plus establishing once and for all the point where the magnitude system is tied down.

Thus, when the visual magnitude system was set up, other systems using detectors of different sensitivities could be related to it through equation 3. Photographic magnitudes were measured on standard blue sensitive plate while photo-visual magnitudes were measured by means of suitable plate and filter combinations to approximate the visual magnitude system. It was agreed that the zero point of the photographic system should be so defined that A0 stars of the Henry Draper Catalogue, with apparent visual magnitudes between +5.5 and +6.5, should have zero color index. Similarly, it becomes possible to measure ultraviolet, red,

or infrared magnitudes and relate them to the visual magnitude by means of a color index which defines the zero point of the new magnitude system. Relative energy distributions in the new system can be determined providing the bandpass characteristics are known for both the visual magnitude determinations and the system magnitude determinations as well as the measure of the energy arriving at the earth from a source measured on one of the standard magnitude systems.

It is natural that efforts would be made to establish photoelectric magnitude systems which agree as closely as possible with the International Photographic and Photo-visual systems. The first attempt at defining a photoelectric system was made by Stebbins and Whitford (Ap. J., 112, pg. 471, 1950) using as standards magnitudes of stars in the north polar sequence (NPS) adopted by the International Astronomical Union (Trans. I.A.U. 1, 69, 1922). Stebbins and Whitford published magnitudes of several stars in the NPS, measured with filters intended to yield magnitudes agreeing with the International system  $m_v$  and  $m_p$ . The resulting photoelectric magnitude system was designated by symbols P and V.

One might have hoped that the P, V system would take its place as a photometric standard suitable for all future work. However, it was pointed out soon after by Johnson (Ap. J., 116, 272, 1942) that, though V magnitudes were entirely satisfactory, rather marked deviations

result when blue magnitudes are measured using filters passing more (or less) of the ultraviolet radiation. In particular, Johnson pointed out that a filter should be used which does not transmit short of  $\lambda$  3800, due to the fact that the Balmer continuum (starting at  $\lambda$  3646) causes a rather strong deviation in the measured magnitudes. Absolute magnitude for intrinsic brightness effects play an equally important role in introducing discrepancies into the observations. It therefore became desirable to redefine a "blue" magnitude, using a filter with a cutoff about  $\lambda$  3800. The cutoff of the filter used in the P system lies at  $\lambda$  3550.

This leads to the establishment of the Johnson-Morgan system (UBV) which is defined in a similar way, but uses stars over the entire sky. Equal energy curves of the photometer response for the UBV system are found in Ap. J., 114, 523, 1951. The system of magnitudes is defined in Ap. J., 117, 313, 1953. The essential definition states that for the average of six selected AOV stars:  $B-V = U-V = 0$ .

It is clear that some compromises must be made to obtain working magnitude systems. If one insists upon refining and revising his magnitude systems, he finds that he is becoming intimately concerned with intensity distributions as functions of wavelength for different kinds of stars. At some point, the law of diminishing returns must set in and it is better to discard the magnitude systems and take up spectrophotometry.

In order to establish the energy related to a given magnitude system, it is necessary to determine the energy arriving at the earth from a known object included in the magnitude system. The International Photo-Visual magnitude of the sun has been determined very accurately by Stebbins and Kron (Ap. J., 126, 373, 1957) to be  $-26.75 \pm 0.03$ , and they have obtained the color index of  $+0.53$ . The distribution of radiation from the spectrum of the sun has been obtained by Moon and Hulbert and is tabulated in the Smithsonian Physical Tables. By determining the bandpass of the photometric system and directly substituting the energy falling within the magnitude band, it is possible to calibrate all photometric systems on the basis of energy sensitivity.

Taking the apparent visual magnitude of the sun as  $-26.73$  (Reference 2)\* and the visual irradiance of the sun calculated in Table I, (page 73) we can determine the visual irradiance for a star of given visual magnitude from the equation:

$$\log \frac{H_{V, \text{sun}}}{H_{V, m_V}} = 0.4(m_V + 26.73)$$

Thus a star whose  $m_V = 1.0$  has a visual irradiance, taking  $H_{V, \text{sun}} = 1.73 \times 10^{-2}$  watts/cm<sup>2</sup>,

$$\begin{aligned} \log H_{V, m_V} &= \log H_{V, \text{sun}} - 0.4(m_V + 26.73) \\ &= -2.722 - 0.4(27.73) \\ &= 13.817 \end{aligned}$$

$$H_{V, 10} = 1.524 \times 10^{-13} \text{ watts/cm}^2$$

---

\* See List of References, page 76.

A star of any other apparent visual magnitude will differ in the visual irradiance from this value by a factor 2.512 for every whole magnitude brighter or fainter than  $m_V = 1.0$ . A star whose  $m_V = +6.0$  will have a visual irradiance:

$$H_{V,6.0} = 1.524 \times 10^{-15} \text{ watts/cm}^2$$

The apparent magnitude of an object in any other spectral band may be determined in much the same way magnitudes of different stars in the same spectral region are obtained. The zero point of such magnitude systems may be chosen in a number of ways. Two methods of assigning such a zero point which have application in this problem are:

1. Assign a zero point on the basis of the irradiance in the two spectral regions so that, for instance, a star will have an apparent magnitude of 1.0 in any spectral band providing there is an irradiance in that band of  $1.524 \times 10^{-13}$  watts/cm<sup>2</sup>.
2. Choose a standard temperature star and assign for that star a color index, or difference between the visual magnitude and the other kind of magnitude, of zero.

The second method is that used in astronomy because of the variation in spectral bandpass characteristics from one magnitude system to another. Also, in astronomy the objects studied most often photometrically do not deviate very far from having similar irradiances in the visual region and the photographic region so that color indices do not fluctuate wildly as the temperature changes over a very wide range. In most stellar objects

observed in the 8 to 14 micron range the relative irradiance ( $H_z/I_V$ ) will vary over three orders of magnitude. If the infrared magnitudes are calibrated with a zero point having the same irradiance as the visual magnitude, the spectral type of the star having such a condition will be just hotter than 2000°. In the tables that follow it was decided to maintain the astronomical definition of magnitude zero points and assign to the infrared magnitudes a zero point equal to the irradiance of an A0 V star,  $T_e = 11,000^\circ\text{K}$ .

The color indices for the 7.5 to 13.5 micron region are given as a function of spectral type in Table II, based upon the assumption that the stars radiate in all regions as blackbodies.

TABLE I  
CALIBRATION OF VISUAL MAGNITUDE  
IN ENERGY UNITS

$\mu$ (microns)	R	E (cal/cm <sup>2</sup> /min)	E' (watt/cm <sup>2</sup> /μ)	RE	RE'
.475	.000	.0312	.220	.00000	.000
.485	.057	.0311	.203	.00177	.0115
.495	.248	.0306	.204	.00758	.0501
.505	.547	.0299	.197	.01635	.1077
.515	.819	.0290	.189	.02375	.1547
.525	.965	.0283	.192	.02828	.1854
.535	.972	.0279	.197	.02711	.1915
.545	.940	.0277	.198	.02606	.1860
.555	.865	.0274	.192	.02371	.1661
.565	.766	.0271	.189	.02078	.1448
.575	.663	.0268	.187	.01776	.1239
.585	.561	.0264	.185	.01482	.1038
.595	.457	.0260	.183	.01188	.0836
.605	.364	.0255	.179	.00928	.0652
.615	.274	.0251	.176	.00688	.0484
.625	.224	.0245	.172	.00549	.0385
.635	.154	.0240	.168	.00370	.0259
.645	.084	.0234	.164	.00196	.0137
.655	.045	.0229	.160	.00133	.0072
.665	.038	.0224	.157	.00085	.0060
.676	.031	.0219	.153	.00068	.0047
.685	.024	.0213	.150	.00051	.0036
.695	.017	.0208	.146	.00035	.0225
.705	.011	.0203	.142	.00022	.0016
.715	.000	.0200	.139	.00000	.0000
				$\Sigma RE = .24980^*$	$\Sigma RE' = 1.7264^{**}$

\* 0.2498 cal/cm<sup>2</sup>/min = 1.74 x 10<sup>5</sup> ergs/cm<sup>2</sup>/sec.

\*\* 1.7264 watt/cm<sup>2</sup>/μ = 1.726 x 10<sup>5</sup> ergs/cm<sup>2</sup>/sec.

R Johnson-Morgan (Ref. 1)  
E Moon, (Ref. 3) Hulbert (Ref. 4)  
E Johnson, F. (Ref. 5)

TABLE II

Spectral Type	V	IV	III	II	I
B0	25000				
B1	22500				
B2	20300				
B3	18000				
B5	15600				
B8	12800				
B9	11800				
A0	11000				
A1	10300				
A2	9700				
A3	9100				
A5	8700				
A7	8100				
F0	7600				
F2	7000				
F5	6600	6540	6470	6340	6200
F6	6390	6210	6020	5910	5800
F8	6150	5890	5620	5460	5300
G0	6000	5750	5300	5150	5000
G2	5730	5350	4990	4770	4600
G5	5520	5080	4650	4470	4290
G8	5320	4870	4440	4220	4000
K0	5120	4650	4200	4010	3820
K1	4920	4450	4000	3850	3700
K2	4760	4280	3810	3700	3590
K3	4610		3660	3540	3430
K5	4400		3550	3430	3320
K6	4000				
M0	3600		3340	3270	3210
M1	3400		3200	3150	3100
M2	3200		3090	3070	3050
M3		2980			
M4		2850			
M5		2710			
M6		2600			
M7					
M8					

Hynek "Astrophysics" - Morgan-Keenan article.

TABLE III

Spectral Type	V	IV	III	II	I
O-B0	-0.20				
B0	-0.20				
B2	-0.20				
B3	-0.20				
B5	-0.20				
B8	-0.12				
B9	-0.08				
A0	0.00				
A1	+0.10				
A2	+0.21				
A3	+0.35				
A5	+0.45				
A7	+0.62				
F0	+0.80				(+0.90)
F2	+1.00				(+1.10)
F4	(+1.10)				(+1.30)
F5	+1.20	+1.23	+1.28	+1.34	+1.42
F6	+1.31	+1.40	+1.50	+1.61	+1.68
F8	+1.45	+1.62	+1.80	+1.94	+2.09
G0	+1.56	+1.74	+2.09	+2.24	+2.35
G2	+1.75	+2.03	+2.39	+2.62	+2.83
G5	+1.88	+2.28	+2.74	+3.00	+3.28
G8	+2.04	+2.51	+3.03	+3.32	+3.66
K0	+2.22	+2.75	+3.40	+3.61	+3.92
K1	+2.45	+3.00	+3.65	+3.89	+4.12
K2	+2.62	+3.26	+3.94	+4.12	+4.28
K3	+2.80	(+3.50)	+4.48	+4.32	+4.52
K5	+3.10	(+3.75)	+4.34	+4.50	+4.74
K6	+3.65				
M0	+4.26		+4.71	+4.85	+4.96
M1	+4.60		+5.00	+5.12	+5.20
M2	+5.00		+5.20	+5.25	+5.34
M3	(+5.40)	(+5.45)	+5.50		
M4	(+5.65)		+5.78		
M5	(+5.90)	(+6.00)	+6.15		(+6.50)
M6	(+6.20)	(+6.32)	+6.48	(+6.60)	(+6.80)
M7	(+6.40)		(+6.80)		
M8	(+6.60)		(+7.10)		

REFERENCES

1. Johnson, H.L. and Morgan, W.W. Ap. J. 114, 523, 1951.
2. Stebbins, J., and Kron, G. Ap. J. 126, 273, 1957.
3. Moon, P., Journ. Franklin Inst. 230, 583, 1940.
4. Hulbert, E.O., JOSA 37, 405, 1947.
5. Johnson, F.S., J. Meteorology 11, 431, 1954.
6. Haynie, W. et al., Semi Annual Report Contract DA-30-069-ORD-2803,  
Jan 1960.

APPENDIX B

COMPARISON OF COLOR INDEX FOR 3.0-4.0 MICRON REGION  
WITH THAT FOR 7.5-13.5 MICRON REGION

It can be noted from the plots of limiting apparent magnitude in Figure 16 that the similarity between the color indices of stars in the two wavelength regions, 3.0-4.0 microns and 7.5-13.5 microns was quite striking. In ordinary stellar photometry the color measurements, made in closely neighboring regions of the spectrum, tend to differ from each other rather markedly. It was rather surprising to find that two color systems having spectral "lever arms" differing by a factor of 3 should have so nearly the same indices.

The values of the two system indices are computed as accurately as possible using the Teddington Slide Rule in the range 2,000° to 12,000°, the results being plotted in Figure 16. The reason for the similarity between the two systems lies in the fact that in the temperature range chosen the two spectral regions lie well to the longward of the peak of the Planck curve and therefore vary in much the same proportion as the temperature changes. Since the colors are expressed in magnitudes and arbitrarily adjusted to a common zero point, the relative changes due to temperature alone tend to produce similar color indices. The values of color index for these two spectral regions will begin to deviate from each other when the temperature drops below about 1500°K.

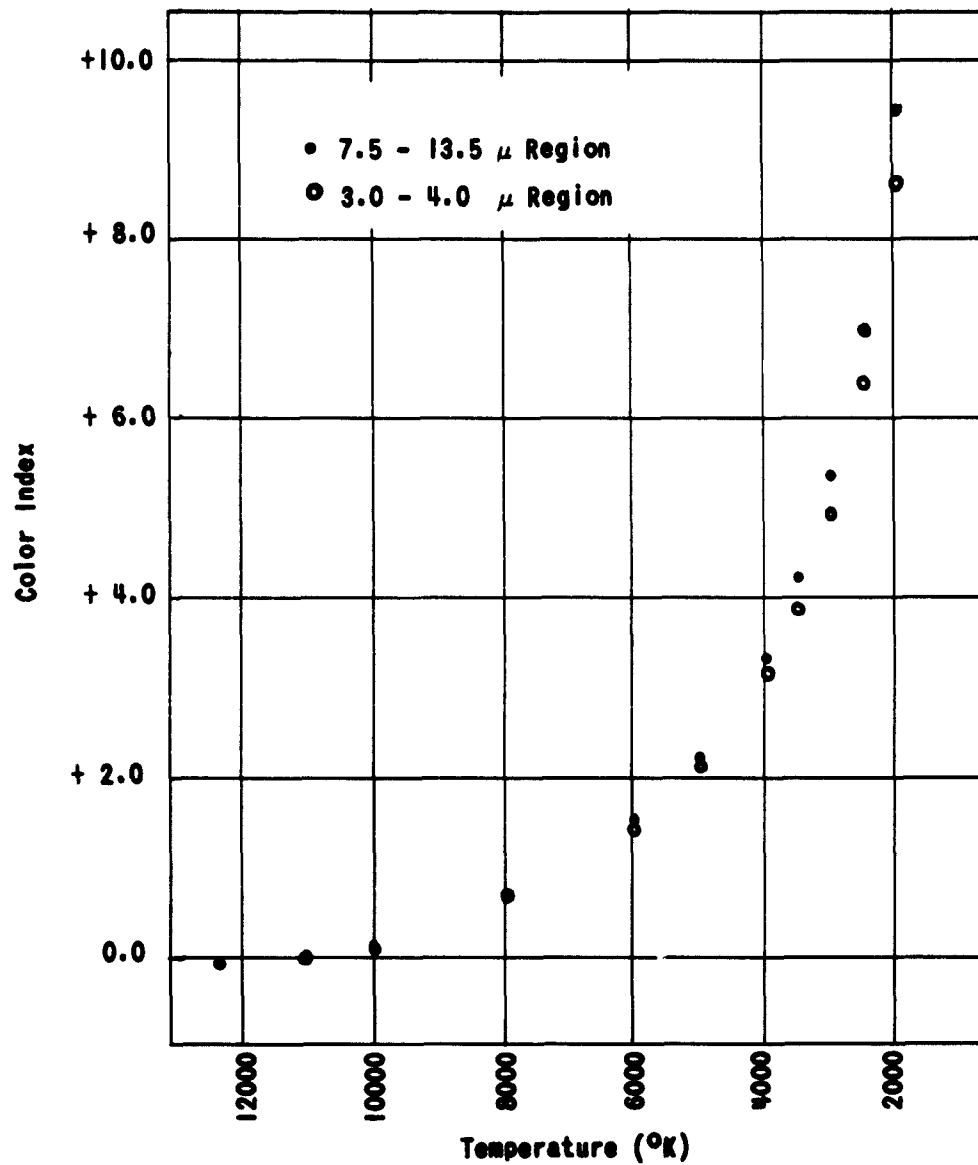


Figure 16. COMPARISON OF INFRARED COLOR INDEXES

APPENDIX C

List of Stars Brighter than  
Apparent Visual Magnitude +6.0  
and Apparent z-Magnitude 0.0

TABLE I

	$\alpha_{1950}$	$\delta_{1950}$	Sp.T.	$m_v$	Z.I.	$m_s$	Star Designation
1	0 12	-08 04	M4 III	5.4	+5.8	-0.4	120
2	0 12	+19 56	M2 III	4.9	+5.2	-0.3	122 X Peg
3	0 12	-19 13	M1 III	4.7	+5.0	-0.3	123
4	0 17	-09 06	M3 III	3.8	4.2	-0.4	177 4 Cet
5	0 19	-20 20	M5 III	5.5	+6.2	-0.7	200 7 Cet
6	0 25	+17 37	M3 III	4.6	+5.5	-0.9	250 7V Peg
7	0 26	-33 17	M5 V	5.0	+5.9	-0.9	251 9 Sol
8	0 37	+30 25	M4 III	3.5	4.2	-0.7	357 8 And
9	0 38	+56 16	07 III	2.5	2.9	-0.4	364 9 Cas
10	0 41	-18 16	06 III	2.2	2.8	-0.6	396 8 Cet
11	0 44	+15 12	M4 III	5.6	+5.8	-0.2	427
12	0 52	-63 09	M5 V	5.6	+5.9	-0.3	507
13	1 06	-10 27	M1 III	3.6	3.6	0.0	660 9Cet
14	1 07	+35 21	M0 III	2.4	4.7	-2.3	666 8 And
15	1 35	+48 23	M2 III	3.8	3.9	-0.1	910 9 Per
16	1 44	-51 04	M5 V	5.5	+5.9	-0.4	999
17	1 58	-08 46	M5 III	5.7	+6.2	-0.5	1108
18	2 01	+42 05	M3 III	2.3	4.2	-1.9	1133 7 And
19	2 04	+23 14	M1 III	2.2	3.6	-1.4	1160 8 Ari
20	2 17	-03 12	M6 III	2.0 max.	6.5	-4.5	1301 9 Cet
21	2 34	+34 03	M4 III	5.4	5.8	-0.4	1473 8 Tri
22	2 47	+55 41	M4 I	3.9	4.6	-0.7	1584 9 Per
23	3 00	+03 54	M2 III	2.8	+5.2	-2.4	1688 8 Cet
24	3 44	-12 15	M2 III	4.6	5.2	-0.6	2121 7 Eri
25	3 45	+65 22	M1 III	4.7	5.0	-0.3	2146
26	4 00	-62 18	M5 V	4.5	+5.9	-1.4	2304 7 Aps
27	4 32	-08 20	M3 III	5.4	5.5	-0.1	2679 8 Tau
28	4 33	+16 25	M5 III	1.1	+4.3	-3.2	2689
29	4 38	-19 46	M4 III	4.5	5.8	-1.3	2747 4 Aur
30	4 54	+33 05	M3 III	2.9	4.2	-1.3	2923 8 Lep
31	4 57	-24 53	M6 V	5.5	6.2	-0.7	2957
32	5 07	-63 28	M5 V	5.2	5.9	-0.7	3044
33	5 09	-11 55	M6 III	5.9	6.5	-0.6	3079
34	5 13	+45 57	01 III	0.9	+2.2	-2.0	3121 8 Aur
35	5 29	+18 34	M2 I	4.7	5.3	-0.6	3253
36	5 46	+37 18	M1 III	5.0	5.0	0.0	3626 9 Aur
37	5 49	-35 47	M1 III	3.2	3.6	-0.4	3644 8 Ocl
38	5 52	+07 24	M2 I	0.1	+5.34	-5.24	3679 8 Ori
39	5 53	+20 10	M6 III	5.2	+7.1	-1.9	3683 8 Ori
40	5 56	+45 56	M3 III	4.6	5.5	-0.9	3733 7 Aur
41	6 11	-65 35	M4 V	4.9	5.6	-0.7	3930 9 Dor
42	6 12	+22 31	M3 III	3.1	5.5	-2.4	3940 9 Gem
43	6 13	+61 32	M3 III	5.3	5.5	-0.2	3962
44	6 20	-02 10	M5 III	6.0	6.2	-0.2	4047 7 Mon
45	6 23	-52 40	PO I	-0.9	+0.8	-1.7	4091 8 Car
46	6 43	-16 39	A2 V	-1.6	+0.2	-1.8	4392 8 Gem
47	6 52	-24 07	M5 I	4.1	4.7	-0.6	4521
48	6 55	-48 39	M3	4.9	5.5	-0.6	4568
49	7 00	-51 20	M3	5.0	5.5	-0.5	4621
50	7 00	-27 52	M0 I	3.7	5.0	-1.3	4625 8 UMa

TABLE I

	$\alpha_{1950}$	$\delta_{1950}$	Sp. T.	$m_v$	Z.I.	$m_z$	Star Designation	
51	7 06	-26 19	G3 I	2.0	+3.0	-1.0	4704	$\delta$ Cha
52	7 12	-44 33	M5	3.4	6.2	-2.8	4782	$\lambda$ Pup
53	7 15	-27 47	M3 III	4.8	5.5	-0.7	4814	
54	7 15	-37 00	K5 V	2.7	3.1	-0.4	4825	$\tau$ Pup
55	7 21	+82 31	M4 III	4.7	5.8	-1.1	4906	$\nu$ Cam
56	7 32	-14 25	M3 III	5.1	5.5	-0.4	5045	
57	7 37	+05 21	F3 V	0.5	+1.0	-0.5	5099	$\alpha$ CMi
58	7 42	+28 09	O8 III	1.2	+3.0	-1.8	5166	$\beta$ Cam
59	7 59	-60 27	M3	5.1	5.5	-0.4	5339	
60	8 06	-32 32	M4	5.4	5.8	-0.4	5368	
61	8 10	-39 28	M0	4.4	4.7	-0.3	5434	
62	8 22	-59 21	M0 V	1.7	+2.2	-0.5	5516	$\epsilon$ Car
63	8 22	-77 19	K5	4.3	4.3	0.0	5555	$\beta$ Cha
64	9 06	-43 14	K4 I	2.2	4.6	-2.4	5989	$\lambda$ Vel
65	9 08	+31 10	M6 III	5.5	6.5	-1.0	6007	$\mu$ , $\nu$ Cnc
66	9 14	-44 03	M2	5.0	5.2	-0.2	6055	
67	9 15	-57 20	K5	4.2	4.3	-0.1	6058	
68	9 25	-08 26	K5 III	2.2	4.3	-2.1	6136	$\alpha$ Hya
69	9 27	-35 44	M0	4.6	4.7	-0.1	6150	$\epsilon$ Ant
70	9 31	-62 34	M5 III	5.6	6.2	-0.6	6189	R Car
71	9 43	+34 45	M8 III	6.0	7.1	-1.1	6269	RL Mi
72	9 43	+57 22	M3 III	5.4	5.5	-0.1	6273	
73	9 45	+11 40	M8 III	4.4	7.1	-2.7	6288	R Leo
74	9 50	+26 15	K3 III	4.1	4.2	-0.1	6325	$\mu$ Leo
75	10 17	+20 06	K1 III	2.6	3.6	-1.0	6502	$\gamma$ Leo
76	10 30	-72 58	M1	4.9	5.0	-0.1	6601	
77	10 35	-27 09	M2 III	5.1	5.2	-0.1	6629	
78	10 37	-58 55	M1	4.8	5.0	-0.2	6642	
79	10 42	-60 18	M1	4.5	5.0	-0.5	6683	
80	10 47	-15 56	K3 III	3.3	4.2	-0.9	6726	$\nu$ Hya
81	10 53	+06 27	M5 III	6.0	6.2	-0.2	6772	
82	10 59	-02 13	M1 III	5.0	5.0	0.0	6812	
83	11 01	+62 01	G7 III	2.0	+2.9	-0.9	6819	$\alpha$ UMa
84	11 07	+44 46	K1 III	3.6	3.6	-0.4	6861	$\beta$ UMa
85	11 12	+23 22	M2 III	4.9	5.2	-0.3	6901	
86	11 16	+33 22	K3 III	3.7	4.2	-0.5	6924	$\nu$ UMa
87	11 30	-30 49	M2	5.2	5.2	0.0	7027	
88	11 36	+08 25	M6 III	5.5	6.5	-1.0	7072	
89	11 46	-66 32	M2	4.7	5.2	-0.5	7112	$\mu$ Mas
90	12 08	-22 21	K3 III	3.2	4.2	-1.0	7289	$\epsilon$ Trv
91	12 15	-67 41	M6 IV	4.2	+6.3	-2.1	7353	$\epsilon$ Mas
92	12 17	-18 59	M5 III	5.9	6.2	-0.3	7389	R Crv
93	12 28	+69 29	M4 III	5.2	5.8	-0.6	7523	
94	12 28	-56 50	M4 III	1.6	+5.8	-4.2	7528	$\gamma$ Cru
95	12 53	+47 28	M8 I	6.0	7.3	-1.3	7724	
96	13 04	+22 53	M5 IV	5.9	6.0	-0.1	7801	
97	13 27	-23 01	M7 III	3.5	6.8	-3.3	8006	R Hya
98	13 29	-06 00	M3 III	4.8	5.5	-0.7	8020	
99	1330	-06 56	M7 III	6.0	6.8	-0.8	8027	S Vir
100	13 39	+54 56	M2 III	4.8	5.2	-0.4	8093	

TABLE I

	$\alpha$ 1950	$\delta$ 1950	Sp.T.	$m_v$	Z.I.	$m_s$	Star Designation
101	13 46	-34 12	M6 IV	4.4	6.3	-1.9	8152
102	13 47	+16 03	M0 III	4.3	4.7	-0.4	8159 $\nabla$ Boo
103	13 50	+34 41	M2 III	5.0	5.2	-0.2	8184
104	14 04	-26 27	K3 III	3.5	4.2	-0.7	8270 $\nabla$ Hy
105	14 04	-36 07	G9 III	2.3	3.2	-0.9	8272 $\nabla$ Cen
106	14 08	-16 04	M3 III	5.1	5.5	-0.4	8300
107	14 13	+19 27	K0 III	0.2	+3.4	-3.2	8341 $\alpha$ Roo
108	14 30	+30 35	K3 III	3.8	4.2	-0.4	8475 $\rho$ Roo
109	14 36	-60 38	OL V	0.1	+1.8	-1.7	8517 $\alpha$ Cen
110	14 43	+27 17	K0 III	2.7	3.4	-0.7	8567 $\epsilon$ Roo
111	14 51	+74 22	K5 III	2.2	4.3	-2.1	8644 $\rho$ UMa
112	15 19	+31 33	M7 III	5.8	6.8	-1.0	889C $\rho$ CrB
113	15 24	+59 08	K3 III	3.5	4.2	-0.7	8925 $\epsilon$ Dra
114	15 34	-27 58	K5 III	3.8	4.3	-0.5	9005 $\nabla$ Lib
115	15 35	-42 24	M0	4.3	4.7	-0.4	9016 $\omega$ Lup
116	15 42	+06 35	K2 III	2.8	3.4	-0.6	9079 $\alpha$ Ser
117	15 53	+43 17	M3 IV	5.5	5.5	0.0	9163
118	15 57	+26 04	QqM3	2.0	5.5	-3.5	9203 $\tau$ CrB
119	16 13	-53 14	M3	5.4	5.5	-0.1	9349
120	16 16	+59 53	M4 III	5.6	5.8	-0.2	9392
121	16 26	-26 19	M1 I	1.2	+5.2	-4.0	9479 $\alpha$ Sco
122	16 27	+41 59	M6 III	5.0	6.5	-1.5	9485
123	16 33	-35 09	M0 III	4.3	4.7	-0.4	9541
124	16 43	-68 56	K5	1.9	+4.3	-2.4	9640 $\alpha$ Tau
125	16 47	-34 12	G9 III	2.4	3.2	-0.8	9669 $\epsilon$ Sco
126	16 50	+15 01	M5 III	5.9	6.2	-0.3	9696 $\epsilon$ Her
127	16 51	-42 17	K5 III	3.8	4.3	-0.5	9719 $\gamma$ Sco
128	16 52	-45 01	M6 III	6.0	6.5	-0.5	9735 RS Sco
129	16 53	-30 30	M6 III	5.0	6.5	-1.5	9756 RR Sco
130	16 56	-53 05	M1	5.2	5.0	-0.8	9777 $\epsilon$ Ara
131	17 01	+14 10	M3 III	5.1	5.5	-0.4	9831
132	17 12	+14 27	M5 I	3.5	6.5	-3.0	9944 $\alpha$ Her
133	17 13	+36 52	K5 III	3.4	4.3	-0.9	9955 $\nabla$ Her
134	17 41	+04 35	K1 III	2.9	3.6	-0.7	10239 $\rho$ Oph
135	17 54	-41 43	M1	4.9	5.0	-0.1	10380
136	17 54	+37 15	K1 I	4.0	4.1	-0.1	10385 $\nabla$ Her
137	17 55	+51 30	K5 III	2.4	4.3	-1.9	10394 $\gamma$ Dra
138	18 10	+31 23	M3 III	5.0	5.5	-0.5	10658
139	18 18	-29 51	K2 III	2.8	3.9	-1.1	10810 $\delta$ Sag
140	18 19	-61 31	M1	4.2	5.0	-0.8	10823 $\gamma$ Pav
141	18 20	+49 06	M2 III	5.1	5.2	-0.1	10854
142	18 25	-25 27	K1 III	2.9	3.6	-0.7	10927 $\lambda$ Sag
143	18 32	-08 17	K5 III	4.1	4.3	-0.2	11039 $\alpha$ Sct
144	18 36	+08 47	M6 III	5.9	6.5	-0.6	11092 $\kappa$ Oph
145	18 36	-43 14	M4	5.4	5.8	-0.4	11093
146	18 53	+36 50	M4 III	4.5	5.8	-1.3	11369 $\zeta$ Lyr
147	18 55	-21 10	K1 III	3.6	0.0	0.0	11399 $\gamma$ Sgr
148	19 04	-27 45	K1 III	3.4	3.6	-0.2	11558 $\nabla$ Sgr
149	19 04	+08 09	M7 III	5.1	6.8	-1.7	11562 $\eta$ Scl
150	19 44	+10 29	M4 III	2.8	4.3	-1.5	12137 $\gamma$ Aql

TABLE I

	$\alpha$ 1950	$\delta$ 1950	Sp.T.	$m_v$	Z.I.	$m_z$	Star Designation	
151	19 49	+32 47	M7 III	2.3	6.8	-4.5	12201	X Cyg
152	19 53	-29 20	M5 III	5.5	6.2	-0.7	12265	RR Sge
153	19 56	+19 21	M0 III	3.7	4.7	-1.0	12320	7 Sgr
154	19 58	-59 31	M6	5.1	6.5	-1.4	12337	
155	19 58	+17 23	M4 III	5.6	5.8	-0.2	12341	
156	20 12	+46 53	K1 I	4.0	4.1	-0.1	12595	o Cyg
157	20 14	+47 34	K5 I	4.2	4.7	-0.5	12638	
158	20 43	+17 54	M6 I	5.6	6.8	-1.2	13009	v Del
159	20 44	+33 47	K0 III	2.6	3.4	-0.8	13020	e Cyg
160	20 46	-46 25	M1	4.9	5.0	-0.1	13052	y Ind
161	20 51	-58 39	K2	3.7	3.9	-0.2	13108	B Ind
162	21 09	-70 20	M2	5.1	5.2	-0.1	13315	o Pav
163	21 09	+68 17	M7 III	5.5	6.8	-1.3	13320	T Cep
164	21 13	-15 23	M3 III	5.5	5.5	0.0	13361	
165	21 24	-69 43	M6	5.5	6.5	-1.0	13486	SX Pav
166	21 28	+23 25	M1 III	4.8	5.0	-0.2	13515	
167	21 34	+45 09	M4 III	5.0	5.8	-0.8	13572	w Cyg
168	21 42	+09 39	M0 I	2.5	3.4	-0.9	13654	e Peg
169	21 42	+58 33	M2 I	3.6	5.3	-1.7	13658	u Cep
170	22 02	+62 53	M5 III	5.5	6.2	-0.7	13871	
171	22 03	-39 47	M0	4.6	4.7	-0.1	13877	A Cru
172	22 06	-34 17	M2	5.1	5.2	-0.1	13908	
173	22 09	+57 57	K5 I	3.6	4.7	-1.1	13949	y Cep
174	22 14	+37 30	K4 III	4.2	4.2	0.0	14004	
175	22 15	-60 31	K5 III	2.9	4.3	-1.4	14024	a Tuc
176	22 27	-44 00	M4	4.3	5.8	-1.5	14130	
177	22 30	-62 14	M5	4.9	6.2	-1.3	14159	v Tuc
178	22 37	+56 32	M4 III	5.5	5.8	-0.3	14229	
179	22 40	-47 09	M6 V	2.2	6.2	-4.0	14260	B Gru
180	23 01	+27 49	M2 III	2.6	5.2	-2.6	14468	
181	23 08	+08 24	M4 III	5.4	5.8	-0.4	14537	
182	23 14	-08 00	M5 III	5.1	6.2	-1.1	14595	X Aqr
183	23 15	+48 15	M2 III	5.0	5.2	-0.2	14610	
184	23 31	+22 13	M5 III	5.5	6.2	-0.7	14770	
185	23 52	-00 10	M5 III	6.0	6.2	-0.2	14957	
186	23 56	+51 07	M7 III	4.8	6.8	-2.0	14998	R Cass

TABLE II

List of the 26 Brightest Stars in  
the 7.5 to 13.5 Micron Region

	Mr. Wilson Cat. Number	Spectral Type	$m_3$	$m_4$	Remarks
1	3679	M2 I	-5.2	0.1	Betelgeuse (max. $m_3$ )
2	12201	M7 III	-4.5	2.3	X Cygni
3	1301	M6 III	-4.5	2.0	O Ceti (Mira)
4	7528	M4 III	-4.2	1.6	Y Crucius
5	9479	M1 I	-4.0	1.2	Antares
6	14260	M6	-4.0	2.2	$\beta$ Gruis
7	9203	M3	-3.5	2.0	T Corona Borealis
8	8006	M7 III	-3.3	3.5	R Hydrae
9	2689	K5 III	-3.3	1.1	Aldebaran
10	8341	K0 III	-3.2	0.2	Arcturus
11	9944	M5 I	-3.0	3.5	$\alpha$ Hercules
12	4782	M5	-2.8	3.4	$\lambda^2$ Puppis
13	6288	M8 III	-2.7	4.4	R Leonis
14	14468	M2 III	-2.6	2.6	$\beta$ Pegasi
15	9640	K5	-2.5	1.9	$\alpha$ Trianguli Australis
16	5989	K4 I	-2.4	2.2	$\lambda$ Velorum
17	3940	M3 III	-2.4	3.1	$\eta$ Geminorum
18	1688	M2 III	-2.4	2.8	$\alpha$ Ceti
19	666	M0 III	-2.3	2.4	$\beta$ Andromedae
20	6136	K5 III	-2.2	2.2	$\delta$ Hydrae
21	8646	K5 III	-2.1	2.2	$\delta$ Ursa Minoris
22	7353	M6 IV	-2.1	4.2	$\epsilon$ Muscae
23	3121	G1 III	-2.0	0.2	Capella
24	14998	M7 III	-2.0	4.8	R Cassiopeiae
25	10394	K5 III	-1.9	2.4	$\gamma$ Draconis
26	1133	M8 III	-1.9	5.2	U Orionis

A number of stars observed in 1928 by Pettit and Nicholson appear on our list. Some of them are compared in Table III. It appears that Pettit and Nicholson were unable to observe as much energy with their thermocouple as is indicated by the black body calculations. This could be due to a lack of sensitivity in the long wavelength window or an actual decrease in infrared emission by the stars.

TABLE III

Comparison of Pettit and Nicholson Observed  
Heat Indices and Computed Z.I.

	MK	T <sub>P-N</sub>	H.I.	Computed Color Index
α Tau	K5 III	3120	+1.66	+4.4
γ Ura	K5 III	3160	+1.48	+4.4
β And	M0 III	3000	+1.92	+4.7
α Sco	M1 I	2660	+2.54	+5.2
α Ori	M2 I	2640	+2.59	+5.3
η Gem	M3 III	2700	+2.6	+5.5
ρ Per	M4 III	2550	+3.0	+5.8
σ Leo	M5 III	2400	+4.18	+6.0
ο Cet	M6 III	2540	+3.8	+6.2
X Oph	M6 III	2260	+5.0	+6.2
R Can	M7 III	2450	+4.7	+6.8
R Leo	M8 III	2260	+5.8	+7.1

DISTRIBUTION LIST

<u>Copy</u>	<u>Copy</u>
<p>Commanding Officer Army Rocket and Guided Missile Agency Redstone Arsenal, Alabama ATTN: ORDER-REA</p>	<p>MIT Lincoln Laboratory Box 73 Lexington 73, Massachusetts ATTN: D. E. Dustin</p> <p style="text-align: right;">25</p>
<p>Contracting Officer New York Ordnance District 770 Broadway, New York 2, N. Y. ATTN: ORDER-O-TA</p>	<p>Radio Corporation of America Moorestown, New Jersey ATTN: Mr. Molthrop</p> <p style="text-align: right;">26</p>
<p>Aerojet-General Corporation Azusa, California</p>	<p>Raytheon Manufacturing Company Missile and Radar Division, Advanced Development Section Bedford, Massachusetts ATTN: Mr. Harold Soule</p> <p style="text-align: right;">27</p>
<p>Aeronutronic Systems, Inc. Division of Ford Motor Company Ford Road, Newport Beach, California ATTN: Dr. Harold Hall</p>	<p>Space Technology Laboratories Ramo Wooldridge Corporation Los Angeles 45, California ATTN: Dr. George Welch</p> <p style="text-align: right;">28</p>
<p>Applied Physics Laboratory 8621 Georgia Avenue Silver Spring, Maryland ATTN: Mr. A. C. Schultheis</p>	<p>Stanford Research Institute Menlo Park, California ATTN: Dr. Scheuch</p> <p style="text-align: right;">29</p>
<p>Armour Research Foundation 10 W. 35th Street Chicago 16, Illinois ATTN: Dr. V. Cushing</p>	<p>Sylvania Electric Products, Inc. 100 First Avenue Waltham 53, Massachusetts ATTN: Dr. J. Thomas Dr. D. Brick</p> <p style="text-align: right;">30 31</p>
<p>ARC Research Laboratory Everett, Massachusetts ATTN: Dr. C. Petty</p>	<p>Commander Air Force Ballistic Missile Division Headquarters, Air Research and Development Command P.O. Box 262 Inglewood, California ATTN: Nose Cone Division, Major Fowler</p> <p style="text-align: right;">32</p>
<p>Barnes Engineering Company 30 Commerce Road Stamford, Connecticut</p>	<p>Commanding Officer Electronics Research Directorate Air Force Cambridge Research Center L. G. Hanscom Field Bedford, Massachusetts ATTN: CRR</p> <p style="text-align: right;">33</p>
<p>Bell Telephone Laboratories Whippany, New Jersey ATTN: J. Schaeffer Dr. D. Ling</p>	<p>Commander Air Research and Development Command Andrews Air Force Base Washington 25, D. C. ATTN: REXES RDFWP RDAMC</p> <p style="text-align: right;">34 35 36</p>
<p>Bendix Aviation Corporation Bendix Products Division 3300 W. Sample Street South Bend, Indiana ATTN: C. M. Shaar</p>	<p>Chief, ARDC Office Room C-107, Building 4408 Redstone Arsenal, Alabama</p> <p style="text-align: right;">37</p>
<p>Convair Division of General Dynamics San Diego, California</p>	<p>Commander Army Ballistic Missile Agency Redstone Arsenal, Alabama ATTN: Technical Library Dr. D. D. Woodbridge</p> <p style="text-align: right;">38 39</p>
<p>Cornell Aeronautical Laboratory 4455 Genesee Street Buffalo 21, New York ATTN: Dr. Graham</p>	<p>24</p>
<p>Hughes Aircraft Company Calver City, California</p>	
<p>Jet Propulsion Laboratory California Institute of Technology 4800 Oak Grove Drive Pasadena, California</p>	

DISTRIBUTION LIST - CONT'D

	<u>Copy</u>		<u>Copy</u>
Commander Army Rocket and Guided Missile Agency Redstone Arsenal, Alabama ATTN: Technical Library	40	Commanding Officer Bureau of Naval Weapons Special Projects Office Navy Department Washington 25, D. C.	55
Commanding General U. S. Army Signal Research and Development Laboratory, Ft. Monmouth, New Jersey ATTN: SIGPM/EL-E	41	Geophysics Corporation of America 700 Commonwealth Avenue Boston 15, Massachusetts	56
Commanding Officer Ballistics Research Laboratory Aberdeen Proving Ground, Maryland ATTN: Dr. B. Karpov	42	Commanding Officer Bureau of Naval Weapons Department of the Navy Washington 25, D. C. ATTN: Dr. Ralph Zirkind	57
Central Intelligence Agency 2430 E. Street N. W. Washington 25, D. C. ATTN: JCR Standard Distribution	43	U. S. Naval Ordnance Laboratory White Oak, Maryland	58
Chief of Ordnance Department of the Army Washington 25, D. C. ATTN: ORDTU	44	Naval Research Laboratory Physics Branch Washington 25, D. C.	59
Chief of Naval Operations Department of the Navy Washington 25, D. C. ATTN: UP-07T	45	Warner Swasey Corporation 34 West 33rd Street New York 1, New York	60
Commanding Officer Diamond Ordnance Fuze Laboratories Washington 25, D. C. ATTN: ORD Library Tech Ref Sec (ORD-TL-06.33) Supporting Research Library	46 47 48	Commanding Officer U. S. Army Signal Missile Support Agency White Sands Missile Range, New Mexico ATTN: SIGMS-EW	61
Commanding Officer Naval Research Laboratory Washington 25, D. C. ATTN: 5365 2021 (Technical Library)	49 50	University of Michigan Radiation Data Library Ann Arbor, Michigan	62
Director of Electronics Office of the Assistant Secretary of Defense Research and Engineering Washington 25, D. C. ATTN: James M. Bridges	51	Commanding Officer Wright-Patterson Air Force Base Wright Field, Ohio ATTN: Mr. W. Kennedy, WCL06-EE	63
Ordnance Technical Intelligence Agency Arlington Hall Station Arlington 12, Virginia ATTN: Major Vickers, ONELI-EW	52	Ohio State University Research Foundation McMillen Laboratory 236 W. 12th Street Columbus, Ohio ATTN: W. E. Mitchell Mr. P. Barnhart	64 65
Headquarters Rome Air Development Center Griffiss Air Force Base, New York ATTN: RCMS, Directorate of Control and Guidance KCOR, Joel S. Greenberg, Advanced Studies Office, DCS/Operations	53 54	Eastman Kodak Company Apparatus and Optical Division Rochester, New York Mr. W. Foran - Mr. A. Simons Mr. E. H. McLaughlin Dr. E. D. McAlister Mr. C. F. Gram Dr. W. E. Raynie Mr. R. G. Whelan Mr. T. Shrader Mr. A. Fraill Technical Library, Lincoln Plant	66 67 68 69 70 71 72 73 74